International Journal of Pharmaceutics 650 (2024) 123685

Contents lists available at ScienceDirect

International Journal of Pharmaceutics

journal homepage: www.elsevier.com/locate/ijpharm

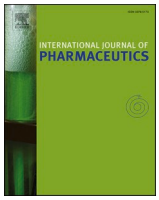

Dexamethasone phosphate and penetratin co-eluting contact lenses: a strategy to enhance ocular drug permeability

Nadia Toffoletto [a,b,*], Madalena Salema-Oom [b], Sara Nicoli [c], Silvia Pescina [c], Felipe M. González-Fernández [c], Carlos A. Pinto [d], Jorge A. Saraiva [d], António P. Alves de Matos [b], Maria Vivero-Lopez [e], Fernando Huete-Toral [f], Gonzalo Carracedo [g], Benilde Saramago [a], Ana Paula Serro [a,b]

[a] Centro de Química Estrutural, Instituto Superior Técnico, University of Lisbon, Av. Rovisco Pais, 1049-001 Lisbon, Portugal
[b] Centro de Investigação Interdisciplinar Egas Moniz (CiiEM), Egas Moniz School of Health & Science, Campus Universitario, 2829-511 Caparica, Portugal
[c] ADDRes Lab, Department of Food and Drug, University of Parma, Parco Area delle Scienze, 27/a, 43124 Parma, Italy
[d] LAQV-REQUIMTE, Department of Chemistry, University of Aveiro, 3810-193 Aveiro, Portugal
[e] Departamento de Farmacología, Farmacia y Tecnología Farmacéutica, I+D Farma (GI-1645), Facultad de Farmacia, Instituto de Materiales (iMATUS) and Health Research Insititute of Santiago de Compostela (IDIS), Universidade de Santiago de Compostela, 15782 Santiago de Compostela, Spain
[f] Ocupharm Research Group, Department of Biochemistry and Molecular Biology, Faculty of Optics and Optometry, Complutense University of Madrid, C/Arcos de Jalón 118, 28037 Madrid, Spain
[g] Ocupharm Research Group, Department of Optometry and Vision, Faculty of Optics and Optometry, Complutense University of Madrid, C/Arcos de Jalón 118, 28037 Madrid, Spain

ARTICLE INFO

Keywords:
Peptide
Penetratin
Anti-inflammatory
Dexamethasone
Drug-eluting contact lens
In vivo ocular biodistribution

ABSTRACT

Contact lenses (CLs) have been suggested as drug delivery platforms capable of increasing the drug residence time on the cornea and therefore its bioavailability. However, when targeting the posterior segment of the eye, the drug released from CLs still encounters the barrier effect of the ocular tissues, which considerably reduces the efficacy of administration. This work aims at the development of CLs able to simultaneously deliver an anti-inflammatory drug (dexamethasone sodium phosphate) and a cell-penetrating peptide (penetratin), the latter acting as a drug carrier across the tissues. Hydroxyethyl methacrylate (HEMA)-based hydrogels were functionalized with acrylic acid (AAc) and/or aminopropyl methacrylamide (APMA) to serve as CL materials with increased affinity for the drug and peptide. APMA-functionalized hydrogels sustained the dual release for 8 h, which is compatible with the wearing time of daily CLs. Hydrogels demonstrated suitable light transmittance, swelling capacity and *in vitro* biocompatibility. The anti-inflammatory activity of the drug was not compromised by the presence of the peptide nor by sterilization. The ocular distribution of the drug after 6 h of CL wearing was evaluated *in vivo* in rabbits and revealed that the amount of drug in the cornea and aqueous humor significantly increased when the drug was co-delivered with penetratin.

1. Introduction

Contact lenses (CLs) have recently emerged as potential platforms for drug delivery to the anterior segment of the eye, and the first commercial drug-eluting CL was introduced to the market in 2022 for the treatment of ocular allergy symptoms (ACUVUE® Theravision® with Ketotifen, by Johnson & Johnson). Therapeutic CLs can provide a sustained release over time, while being a patient-friendly and easily replaceable device (Toffoletto et al., 2021). Moreover, as CLs increase the drug residence time on the cornea (Hui, 2017), they allow for a higher drug bioavailability if compared to commonly used eye drops. Lacrimal fluid renewal, increased post-administration tearing, the anatomical barrier of the ocular tissues and extensive systemic drug absorption are among the causes of a low drug delivery efficiency of eye

* Corresponding author.
E-mail addresses: nadia.toffoletto@tecnico.ulisboa.pt (N. Toffoletto), moom@egasmoniz.edu.pt (M. Salema-Oom), sara.nicoli@unipr.it (S. Nicoli), silvia.pescina@unipr.it (S. Pescina), felipemanuel.gonzalezfernandez@unipr.it (F.M. González-Fernández), carlospinto@ua.pt (C.A. Pinto), jorgesaraiva@ua.pt (J.A. Saraiva), apamatos@egasmoniz.edu.pt (A.P. Alves de Matos), mariavivero.lopez@usc.es (M. Vivero-Lopez), fhueteto@ucm.es (F. Huete-Toral), jgcarrac@ucm.es (G. Carracedo), b.saramago@tecnico.ulisboa.pt (B. Saramago), anapaula.serro@tecnico.ulisboa.pt (A.P. Serro).

https://doi.org/10.1016/j.ijpharm.2023.123685
Received 6 September 2023; Received in revised form 29 November 2023; Accepted 6 December 2023
Available online 10 December 2023

drops (i.e., only ≤ 5 % of the administered drug reaches the target tissues (Maulvi et al., 2015)), which reflects on the multiple daily instillations required (Hsu et al., 2015).

Recent animal studies (Ross et al., 2019; Pereira-da-Mota et al., 2022; Gade et al., 2020) evidenced that small drugs delivered from CLs could also be detected in the vitreous humor and retina, opening the possibility of treating pathologies that affect the posterior segment of the eye without the need for invasive intraocular drug injections. Despite the promising results, the presence of the anatomical ocular barriers still limits the penetration of the drugs through the tissues, thus requiring the release of massive drug doses from the CLs to reach a therapeutic concentration in the posterior segment.

Much effort has been made to implement strategies that allow to increase drug transport across the ocular barriers, and therefore the efficiency of topical administration, when the interior of the eye is the target (Moiseev et al., 2019; Ghosh et al., 2018). Among these, peptides have gained interest as potential drug carriers (Thareja et al., 2021; Pescina et al., 2018). Cell penetrating peptides (CPPs) are non-toxic short-chain peptides, which are named as such due to their ease of internalization across cellular membranes. They have been recently proposed as delivery enhancers of a variety of ocular therapeutic agents including small drugs and macromolecules, such as anti-fungal drugs (Jain et al., 2015; Amit et al., 2019), anti-inflammatory drugs (Gonzalez-Pizarro et al., 2019), growth factors (Wang et al., 2010), anti-VEGF (de Cogan et al., 2017), recombinant proteins (Johnson et al., 2010), siRNA and plasmid DNA (Johnson et al., 2008). Both physical and covalent drug-peptide associations have been reported in the literature. The possibility of simply co-delivering the carrier and the cargo represents an advantageous option, since no drug modification is required.

A therapeutic CL able to simultaneously release a carrier peptide (either penetratin or kyotorphin) and dexamethasone sodium phosphate (DexSP) was developed in the current study with a dual purpose: provide a sustained drug release throughout the day and increase the permeability of DexSP across the ocular tissues. The combination of these two effects is expected to significantly improve the efficacy of DexSP treatment, while maintaining the low invasiveness of topical drug administration.

Dexamethasone is a widely used corticosteroid, used in ophthalmic applications in the form of injections (e.g., Dexycu® by Icon Bioscience, for the treatment of postoperative inflammation) or implants (e.g., Ozurdex® by Allergan, for the treatment of uveitis and macular edema). DexSP, the phosphate ester of Dex, is characterized by a much higher solubility in aqueous media, and therefore it is commonly used for topical administration in the form of eye drops (generally in a concentration of 1 mg/mL).

Penetratin (RQIKIWFQNRRMKWKK-NH_2) is a well-known natural CPP derived from the antennapedia of Drosophila melanogaster (Pescina et al., 2020). It was shown to increase drug transport across biological membranes both when forming a covalent complex with the cargo (Xia et al., 2012) and when simultaneously delivered in solution (Cohen-Avrahami et al., 2012; Frøslev et al., 2022; Kristensen et al., 2015). Kyotorphin is a small endogenous neuropeptide, which, due to its analgesic effect, has been investigated as a safer alternative to opioids in pain relief applications. Used in its amidated form (YR-NH_2), it was shown to cross the blood–brain barrier in rats (Ribeiro et al., 2011).

Ex vivo permeability tests were performed on porcine conjunctivas to select the most promising drug-peptide combination. Hydroxyethyl methacrylate (HEMA) based CLs incorporating functional monomers (i.e., N-(3-aminopropyl) methacrylamide (APMA) and/or acrylic acid (AAc)) were designed to tune the amount of drug and peptide loaded and their release kinetics. The obtained devices were characterized in terms of their physical properties and biocompatibility *in vitro*. In view of a clinical use of the device, the effect of pressure-assisted thermal sterilization was assessed. Finally, *in vivo* tests on rabbits were conducted to evaluate the effectiveness of the strategy for the first time.

2. Materials and methods

2.1. Materials

Dexamethasone sodium phosphate (DexSP, CAS 2392–39-4; 516.4 g/mol) and dexamethasone (Dex, CAS 50–02-2; 392.5 g/mol) were purchased from Carbosynth (Compton, UK). Penetratin trifluoroacetic salt (PEN, CAS 214556–79-3; 2245.8 g/mol) was purchased from Bachem AG (Bubendorf, Switzerland). Custom-made amidated kyotorphin (KTP-NH_2) was purchased from INTAVIS Peptide Services GmbH (Tübingen, Germany). The structures of the studied molecules are presented in Fig. S1.

Ethylene glycol dimethacrylate (EGDMA, CAS 97-90-5), 2,2′-azobis (isobutyronitrile) (AIBN, CAS 78-67-1), 2-hydroxyethyl methacrylate (HEMA, CAS 868-77-9) and N-(3-aminopropyl) methacrylamide hydrochloride (APMA, CAS 72607-53-5) were purchased from Sigma-Aldrich (Steinheim, Germany). Acrylic acid (AAc, CAS 79-10-7) was purchased from Alfa Aesar (Kandel, Germany).

Distilled and deionized water (resistivity > 18 MΩcm) was obtained from a Millipore system. Acetonitrile HPLC grade (CAS 75-05-8) was purchased from Carlo Erba Reagents (Val-de-Reuil, France). Phosphate buffer saline (PBS), pH 7.4, was purchased from Sigma–Aldrich (Steinheim, Germany). Phosphate buffer (pH 6.0) was prepared with the following composition: NaOH 1.15 mM (VWR—Leuven, Belgium) and KH_2PO_4 10 mM (ITW Reagents, Barcelona, Spain).

Porcine eyes were obtained from a local slaughterhouse (Macello Annoni S.p.A., Parma, Italy). Eyeballs were enucleated from 10 to 11-month-old animals (Landrance and Large White breeds, 145–190 kg, female and male), transported at 4 °C in PBS and used for *ex vivo* tests within 2–3 h from enucleation.

Human Corneal Epithelial Cells (ATCC PCS-700-010), Corneal Epithelial Cells Basal Medium (ATCC PCS-700-030), Corneal Epithelial Cell Growth Kit (ATCC PCS-700-040) and RPMI-1640 medium (ATCC-30-2001) were purchased from LGC Standards (Barcelona, Spain). THP-1 human monocytes cell line (ATCC TIB-202) was kindly provided by Dr. Nuno Taveira from the University of Lisbon, Faculty of Pharmacy. Fetal bovine serum, penicillin, streptomycin, lipopolysaccharides (LPS) from *Escherichia coli* O111:B4, yellow tetrazolium (3-(4,5-dimethylthiazolyl-2)-2,5-diphenyltetrazolium bromide) (MTT), dimethyl sulfoxide (DMSO, ≥99 %), isopropanol and hydrochloric acid were purchased from Sigma-Aldrich (Steinheim, Germany). IGEPAL® and phorbol 12-myristate 13-acetate (PMA, CAS 16561–29-8) were purchased from Merck (Darmstadt, Germany).

Schirmer test strips were purchased from Contacare Ophthalmics and Diagnostics (Gujarat, India). Propofol injectable solution (10 mg/mL) was purchased from B. Braun VetCare SA (Rubi, Spain), while Dolethal injectable solution (200 mg/mL) was purchased from Vetoquinol Especialidades Veterinarias SA (Madrid, Spain). Glutaraldehyde, sodium cacodylate, osmium tetroxide and propylene oxide were purchased from Sigma-Aldrich (Steinheim, Germany).

2.2. Drug and peptide selection ex vivo

The drug permeability across the porcine conjunctiva and the effect of the presence of peptides (either KTP-NH_2 or PEN) on such parameter were assessed *ex vivo*. Porcine conjunctivas (n ≥ 3) were examined to select a uniform tissue portion, then clamped in Franz diffusion cells (permeation area: 0.2 cm^2) while still attached to the eyeball to simplify tissue handling (Pescina et al., 2019). The conjunctival epithelium was placed facing the donor chamber. After clamping, the eyeball was removed, the receptor chamber was filled with approximately 4 mL of degassed PBS and the Franz cells were placed in a thermostatic bath at 37 °C with magnetic stirring of the receptor chamber. The donor chamber was then filled with 200 μL of drug solution in PBS without peptide (i.e., 500 μg/mL DexSP or 80 μg/mL Dex, due to solubility limitations) or with peptides (i.e., DexSP: KTP-NH_2 in a 1:1 molar ratio;

DexSP: PEN in a 10:1 molar ratio; Dex: PEN in a 10:1 molar ratio) and covered with parafilm to prevent evaporation. When PEN was tested, a molar excess of drug was placed in the donor chamber of the Franz cells to account for the seven theoretical charges of PEN at pH 7.4 and the possibility for a single PEN molecule to simultaneously interact with multiple drug molecules. At each time point (i.e., 0, 0.5, 1, 2, 3 and 4 h), 300 μL of medium was removed from the receptor chamber for analysis of the drug concentration and replaced with fresh PBS. The cumulative amount of drug permeated, normalized for the permeation area, was plotted against time and fitted to a linear least squares regression. The steady state flux, J (μg/cm^{2}s), was obtained as the slope of the regression line. The apparent permeability coefficient, P_{app} (cm/s), was then calculated as the ratio between J and the initial drug concentration (μg/mL) in the donor chamber (Kristensen et al., 2015; Pescina et al., 2019).

DexSP and Dex were quantified using an HPLC/UV–Vis system (Infinity 1260, Agilent Technologies, Santa Clara, CA, USA) fitted with a C18 Novapak® column (3.9 x 150 mm; particle size: 4 μm) (Waters, Ireland). The analysis was performed setting a 50 μL injection volume and 1 mL/min flow rate. The mobile phase for DexSP quantification consisted in a mixture of 0.01 M phosphate buffer (pH 6.0) and acetonitrile in the ratio of 80:20 *v/v*. The mobile phase for Dex was a mixture of water and acetonitrile in a 62:38 *v/v* ratio. DexSP was detected at a wavelength of 242 nm, with a retention time of 2.9 min, while Dex was detected at 246 nm with a retention time of 2.4 min. The HPLC methods were validated for linearity, accuracy and precision in the 0.2–50 μg/mL and 0.2–10 μg/mL concentration range for DexSP and Dex, respectively.

2.3. Hydrogels design and synthesis

Hydrogels were synthesized with the compositions reported in Table 1. HEMA was selected as the backbone monomer of all hydrogels. APMA and/or AAc (Fig. 1) were added to the prepolymer mixture as potential functional monomers due to their high affinity to either DexSP (Toffoletto et al., 2021) or cationic peptides such as PEN (Malakooti et al., 2015), respectively, with the purpose of tuning the drug/peptide amount loaded and the release kinetics. AIBN and EGDMA were added as initiator and crosslinker, respectively.

The prepolymer mixtures were injected into molds made of two silanized glass plates (10 x 10 cm) with a 0.3 mm thick Teflon frame. Thermal polymerization was performed at 60 °C for 24 h. The obtained hydrogel sheets were immersed in distilled water to remove the unreacted monomers. Water was renewed twice a day until the peaks associated with the presence of residual monomers could not be detected by UV–Vis spectrometric analysis of the washing solution. Then, the hydrogel sheets were cut into flat discs with a biopsy puncher (∅ = 14 mm for all samples, unless when explicitly stated otherwise), to resemble the size of commercial CLs. The obtained discs were dried at 40 °C for 24 h prior to storage.

2.4. Drug and peptide loading

Dry hydrogel discs were loaded following a two-phase protocol: first, the discs were soaked into 2 mL of DexSP solution (0.5 mg/mL in PBS) for 3 days at room temperature, followed by soaking into 0.5 mL of a drug + peptide solution (0.5 mg/mL DexSP + 0.5 mg/mL PEN in PBS) for 3 days at 4 °C.

To evaluate the effect of the simultaneous drug and peptide loading when compared to single loading, the hydrogel with the most adequate dual release profile (H3 hydrogel, as will be proved below) was also individually loaded with either DexSP (3 days soaking into 2 mL of 0.5 mg/mL DexSP in PBS at room temperature, followed by 3 days into 0.5 mL of 0.5 mg/mL DexSP in PBS at 4 °C) or PEN (3 days soaking into 0.5 mg/mL PEN in PBS at 4 °C).

Table 1
Composition of the hydrogels tested as potential CL materials.

Code	HEMA	APMA	AAc	AIBN	EGDMA
H1	4.5 mL	–	–	10 mg	0.15 mL
H2	4.5 mL	–	600 mM	10 mg	0.15 mL
H3	4.5 mL	100 mM	–	10 mg	0.15 mL
H4	4.5 mL	100 mM	600 mM	10 mg	0.15 mL

The loading kinetics of DexSP into the hydrogel was previously monitored to optimize the two-phase loading protocol and determine the required total soaking time (Fig. S2). Briefly, a 20 μL aliquot of the DexSP loading solution was collected for quantification every 24 h during the hydrogel soaking period (under the conditions described above) until no variation in the drug concentration was detectable. The short period of peptide stability in solution (Figs. S3 and S4) imposed the shorter soaking period and lower temperature for the second phase of the loading procedure, while the smaller loading volume (0.5 mL) was selected for a cost-effective protocol.

The total amount of drug and peptide loaded into the hydrogel discs, after either single or dual loading, was calculated as the difference in concentration between the loading solution at the end of the loading phase and a control solution stored under the same conditions of the loading solution, but with no hydrogel disc, to eliminate any storage effect on quantification. Quantification was performed with a UV–Vis spectrophotometer (MultiskanGO, ThermoScientific, Porto Salvo, Portugal), measuring the absorbance of DexSP at 242 nm and the absorbance of PEN at 280 nm. Calibration curves were obtained in the 10 – 120 μg/mL and 2 – 125 μg/mL concentration range for DexSP and PEN, respectively. In the case of dual loading, the full spectrum was deconvoluted considering it as the linear combination of the single spectra of the drug and the peptide (Equation (1)), as previously described by Kim and Chauhan (Kim and Chauhan, 2008).

$$Abs_{Dual} = \alpha \bullet Abs_{DexSP} + \beta \bullet Abs_{PEN} \quad (1)$$

Briefly, the constants α and β were determined by a least-square fit between the dual spectrum (Abs_{Dual}) and the individual drug or peptide spectra (Abs_{DexSP} and Abs_{PEN}, respectively) using the function 'fminsearch' in MATLAB (v2019b, The MathWorks Inc., Natick, MA, USA). The procedure assumes that the absorbance spectra are additive and linear in concentration. All drug/peptide loading studies were performed at least in triplicate.

2.5. In vitro release profile

The release profile from the hydrogel discs (n = 3), loaded with DexSP, PEN or both, as described in Section 2.4, was evaluated *in vitro* for 24 h. The discs were removed from the loading solution, rinsed in distilled water to remove the drug/peptide excess from the surface and gently blotted with absorbent paper. Each disc was then immersed in 3 mL of PBS to ensure sink conditions and incubated at 36 °C with 180 rpm shaking. At different time points (i.e., hourly for 8 h and after 24 h), aliquots of 0.3 mL were collected for drug/peptide quantification and were replaced by the same volume of fresh PBS. Drug and peptide quantification was performed by UV–Vis spectrophotometry as described in Section 2.4.

2.6. Physical characterization

The wettability of the hydrogels was determined by the captive bubble method on hydrogel discs which were pre-hydrated in water for 24 h. The samples were placed horizontally in a measuring cell filled with distilled water, then air bubbles (3–4 μL) were formed and released underneath the inferior surface of the hydrogels by using a micrometer syringe with a curved needle. Images were acquired during 60 s using a video camera (JAI CV-A50, Copenhagen, Denmark) mounted on an optical microscope (Wild M3Z, Leica Microsystems, Jena, Germany) and connected to a frame grabber (Data Translation DT3155, Measuring

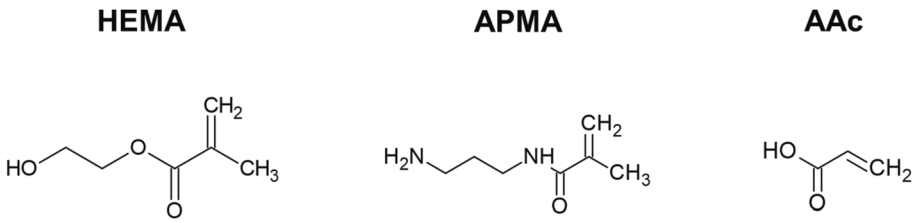

Fig. 1. Molecular structure of the hydrogel monomers: HEMA, selected as the backbone monomer; APMA, used as a functional monomer for interaction with the anionic DexSP, and AAc, used as a functional monomer for interaction with PEN.

Computing Corp., Norton, MA, USA). The measurements were performed over 2 discs for each hydrogel formulation, and 10 bubbles were created for each formulation. The acquisition and analysis of the images were performed using the ADSA-P software (Axisymmetric Drop Shape Analysis Profile, Applied Surface Thermodynamics Research Associates, Toronto, Canada).

The liquid uptake of the hydrogels was evaluated after immersion in the drug + peptide solution. For this, dry hydrogel discs (n = 3) were weighted before soaking and at the end of the dual loading procedure referred to in Section 2.4. The liquid uptake was calculated as in Equation (2), where w_0 and w_t are the weights of the dry and swollen discs, respectively. The liquid uptake of the hydrogels was also evaluated in plain PBS, immersing dry discs (n = 3) at room temperature for 3 days, followed by 3 days at 4 °C.

$$Liquid\ uptake(\%) = \left[\frac{w_t - w_0}{w_0}\right] \bullet 100 \quad (2)$$

The transmittance of the hydrogels (n = 3) was recorded at the end of the drug + peptide loading by UV–Vis spectrophotometry in the 200–700 nm range, to ensure the fulfillment of the optical requirements and prove the suitability of the hydrogels as CL materials.

2.7. Sterilization

Pressure-assisted thermal processing (PATP) was selected as the sterilization method due to the possibility of maintaining low temperatures throughout the process, thus avoiding drug and peptide degradation. PATP is an FDA-approved pasteurization method in the food industry (Wang et al., 2016), and, due to its advantages, it has been recently suggested as an alternative sterilization technique in the medical field (Topete et al., 2020; Daoud-Mahammed et al., 2008).

Hydrogel discs (n = 3) were subjected to PATP either on day 4 or on day 6 of the loading procedure (i.e., at the beginning or the end of the second phase of loading). To perform the procedure, the discs were packed in heat-sealed polyamide/polyethylene bags with 0.5 mL of drug + peptide loading solution (0.5 mg/mL DexSP + 0.5 mg/mL PEN in PBS). The obtained packages were pre-heated at 50 °C for 10 min in a water bath and then placed in a PTFE insulation vessel with a piston containing pre-heated water to perform the procedure. A high-pressure equipment (Hiperbaric 55, Hiperbaric S.A., Burgos, Spain) was used at validated operating conditions (Topete et al., 2020), i.e., 50 °C with a pressure of 500 MPa for 5 min. The effect of PATP on the release profile of the hydrogels was assessed and results were compared to the release profile of non-processed hydrogels.

To evaluate the stability of the drug and the peptide after the sterilization procedure, bags containing solutions of either DexSP or PEN (1 mg/mL) were also subjected to PATP. Circular dichroism (CD) was performed on the PEN solution before and after sterilization, to detect any changes in the peptide secondary structure. Briefly, spectra resultant from three accumulations between 198 and 250 nm were recorded on a JASCO J-720 spectropolarimeter (JASCO, Hiroshima, Japan) using quartz cells with an optical path of 2 mm. The eventual DexSP degradation was instead monitored using a HPLC-UV system as described in Section 2.2.

2.8. In vitro biological characterization

2.8.1. Cytotoxicity

After dual loading with drug and peptide, H3 hydrogel discs (∅ ≈ 10 mm, n = 4, sterilized on day 6 of the loading procedure) were tested for cytotoxicity using primary Human Corneal Epithelial Cells (HCEC). Unloaded sterilized hydrogel discs (n = 4) were also tested to assess the potential toxicity of the material.

Cytotoxicity was evaluated by indirect contact (Toffoletto et al., 2021; Zhang et al., 2016) according to the ISO 10993–5: 2009 standard, placing the hydrogels in cell culture inserts (Transwell®, Corning, Glendale, AZ, USA; 12 mm diameter). Cells were cultured at 37 °C in a humidified 5 % CO_2 incubator with Corneal Epithelial Cells Basal Medium supplemented with a Corneal Epithelial Cell Growth Kit according to the ATCC guidelines. Cell suspension, from passages 2 to 4, was seeded in a 12-well culture plate to obtain 0.7 x 10^5 cells/well and incubated for 24 h at the growth conditions. Then, the culture medium was renewed. Hydrogels were rinsed in sterile PBS, blotted, and transferred into the inserts, and these were placed in the wells. 200 μL of fresh medium was added on top of the hydrogels to ensure complete immersion, to reach a total of 700 μL/well. Negative (cells with HCEC medium) and positive (cells with HCEC medium and 10 % DMSO) control wells (n = 4) were also prepared. After 24 h, inserts were removed, cells were rinsed with PBS and incubated with 400 μL/well MTT solution (0.5 mg/mL MTT in HCEC medium) for 3 h. Then, 600 μL of a formazan-dissolving solution (0.1 % IGEPAL in isopropanol with hydrochloric acid 4 mM) was added to each well. Plates were shaken in a dark environment at room temperature for 1 h. The absorbance was measured at 565 nm in a microplate reader (Infinite® 200 PRO, Tecan, Männedorf, Switzerland). The relative quantification of cell viability was normalized to the negative control.

2.8.2. Ocular irritability test (HET-CAM)

H3 hydrogels (n = 3), loaded with both drug and peptide and sterilized on day 6 of the loading procedure, were evaluated for potential ocular irritation using the Hen's Egg Test on the Chorioallantoic Membrane (HET-CAM) as reported in previous studies (Pereira-da-Mota et al., 2022; Silva et al., 2021). Briefly, fertilized hen's eggs (Sociedade Agrícola da Quinta da Freiria, SA, Portugal) were incubated for 8 days at 37 °C and 60 % RH. Then, each eggshell was cut above the air cell and the inner membrane was exposed. After hydration with 0.9 % NaCl for 30 min, the membrane was detached, thus giving access to the CAM. Hydrogels were placed on the CAM and the time (in seconds) until eventual hemorrhage (t_H), vascular lysis (t_L) or coagulation (t_C) was recorded for 5 min. Solutions of 0.9 % NaCl and 1 M NaOH were used as negative and positive control, respectively. The irritation score (IS) was then calculated as follows (Equation (3)) (Budai et al., 2010):

$$IS = \frac{(301 - t_H) \bullet 5}{300} + \frac{(301 - t_L) \bullet 7}{300} + \frac{(301 - t_C) \bullet 9}{300} \quad (3)$$

Depending on the obtained IS value, the samples were classified as non-irritating ($0 \leq IS \leq 0.9$), slightly irritating ($1 \leq IS \leq 4.9$), moderately irritating ($5 \leq IS \leq 8.9$) or severely irritating ($9 \leq IS \leq 21$).

2.8.3. Anti-inflammatory activity

An *in vitro* anti-inflammatory assay was performed with THP-1 human monocytes to evaluate the effect of (i) the presence of the peptide and (ii) PATP sterilization on the anti-inflammatory activity of DexSP.

THP-1 cells were cultured in suspension at 37 °C in a humidified 5 % CO_2 incubator with RPMI-1640 supplemented with 10 % fetal bovine serum and 1 % penicillin–streptomycin. Cells were seeded in a 24-well culture plate to obtain 7 x 10^4 cells/well. Differentiation of monocytes into macrophages was achieved by adding 600 μL of a 200 nM PMA solution in each well (Lorenzo-Veiga et al., 2020). After incubation for 54 h, the medium was renewed and the cells were exposed overnight to a pre-treatment (Pereira-da-Mota et al., 2022; Olajide et al., 2021; Tomani et al., 2020) with the following solutions: DexSP 20 μM; PEN 10 μM; a combination of DexSP and PEN (20 μM DexSP and 10 μM PEN); a combination of DexSP and PEN after PATP sterilization (20 μM DexSP and 10 μM PEN). Then, after rinsing the cells with PBS, the medium was renewed and cells were stimulated with 100 ng/mL LPS to provoke an inflammatory response. Unstimulated cells, not pre-treated with drug/peptide solutions nor exposed to LPS, were used as negative control, while cells treated with only LPS served as positive control. Each case was prepared in quadruplicate.

After 24 h, cell culture supernatants were collected and stored at −80 °C for quantification of secreted Interleukin 6 (IL-6), an inflammatory mediator. The concentration of IL-6 was analyzed without the need for sample dilution by specific ELISA (RAB0307 by Merck, Darmstadt, Germany), following the manufacturer's instructions.

2.9. In vivo experiments

2.9.1. CLs production

Curved CLs were produced from H3 hydrogel to be tested *in vivo* with rabbits. The composition of H3 hydrogel (Table 1) was modified by doubling the amount of AIBN, the initiator, to ensure a complete polymerization of the thinner CLs within the 24 h of thermal treatment (Pereira-da-Mota et al., 2022). CLs were polymerized inside curved custom-made Teflon molds (10.5 mm diameter, 5.6 mm curvature) with a 0.1 mm Teflon spacer, following the procedure described in Section 2.3. The obtained CLs had the final dimensions of approximately 13 mm diameter, 8 mm curvature, and 0.3 mm thickness in the hydrated state (PBS, pH 7.4). CLs loading was performed as indicated in Section 2.4, except for the volume of the loading solution, which was doubled due to the larger dimensions of the CLs if compared to flat discs. Sterilization was performed as in Section 2.7, on day 6 of the loading procedure. Then, the CLs were stored at −20 °C in the loading solution for a maximum time of 10 days until being used *in vivo*.

The effect of the storage and of the hydrogel modifications (i.e., increased AIBN amount and curved shape) on the drug/peptide release profiles was assessed *in vitro* following the protocol described in Section 2.5. The effect of the hydrogel modifications on the physical properties (i.e., liquid uptake and thermal behavior) was also assessed. The liquid uptake of H3 discs and H3 CLs in PBS was quantified as described in Section 2.6. For the thermal characterization, samples of H3 discs and H3 CLs ($n \geq 3$, dry weight ≈2.5 mg) were dried in a vacuum oven at 40 °C for 72 h and placed in sealed crucibles to be tested through a differential scanning calorimeter (DSC 200 F3 Maia by NETZSCH, Selb, Germany). Thermograms were obtained by heating the samples between 25 °C and 250 °C, at a rate of 10 °C/min, for two cycles. The thermogram of the second cycle was used to determine the glass transition temperature (Tg) of the material (Bhat et al., 2019), which was extrapolated using Proteus Thermal Analysis software (NETZSCH, Selb, Germany).

2.9.2. Study design

In vivo experiments were performed according to the Association for Research in Vision and Ophthalmology (ARVO) Statement for the Use of Animals in Ophthalmic and Vision Research and to the European Directive 2010/63/EU. Protocols were approved by the Ethics Committee for Animal Experimentation of Universidad Complutense de Madrid [Registration number: CEEA-UCM- 4618072022–2022]. The sample size was selected applying the 3Rs principle.

Ten New Zealand white rabbits (male, age 3 months, weight 3.86 ± 0.46 kg) were included in the study. The animals were kept in individual cages in a controlled room (12 h light/dark cycles, 18 °C, 50 % relative humidity), with total access to food and water, for at least one week before the beginning of the experiment. The rabbits were randomly divided into three groups: the first group (4 rabbits) wore CLs loaded with DexSP only; the second group (5 rabbits) wore CLs loaded with DexSP and PEN; the third group (1 rabbit) was set as control for the histological analysis, and did not wear any CL. All animals received the same treatment in both eyes.

A slit lamp examination (VX75, Luneau Technology - Chartres, France) was performed at the beginning of the experiment to exclude the presence of defects on the ocular surface. Then, the CLs were removed from the sterilized bags, rinsed twice with sterile saline solution to remove excess drug on the CL surface, and carefully applied on the rabbit́s eyes, below the nictitating membrane, without local anesthesia. Rabbits were placed in individual restrainers for 6 h, with constant monitoring, to minimize the possibility of CL removal. Due to the low blinking rate, the rabbit́s eyes were kept closed for 1 min every 15 min to prevent the CL from drying. Tear fluid samples were collected at fixed time points (t = 30 min, and hourly until the 6th h) using Schirmer test strips. Briefly, the strips were placed on the palpebral conjunctiva of the lower eyelid for 10 s, keeping the rabbit́s eyes closed during the collection of tears. The volume of the collected samples was recorded as the length of moistened strip, each mm corresponding to 1 μL of tears. Rabbits were euthanized at the end of the experiment by intravenous administration of 0.75 mL/kg of propofol and 0.7 mL/kg of pentobarbital sodium (Dolethal 200 mg/mL).

2.9.3. Drug extraction and quantification

Preliminary *ex vivo* studies were performed to validate the drug extraction method from the ocular tissues. Briefly, samples of thawed porcine ocular tissues (previously stored at −20 °C) were weighted in 1.5 mL Eppendorf® tubes. Then, 20 μL of DexSP stock solution (1 mg/mL DexSP in 90 % ethanol) was applied onto the tissues, allowing for solvent evaporation (González-Fernández et al., 2023). After 1 h, 1 mL of extraction medium was added (i.e., 65 % v/v acetonitrile in water). The aqueous humor and vitreous humor were considered an aqueous phase, and were therefore immersed in pure acetonitrile to reach a final concentration of 65 % acetonitrile in the samples. All samples were sonicated for 10 min and incubated overnight at 4 °C to extract the drug and precipitate the proteins. Then, samples were vortexed for 1 min and centrifuged at 13000 rpm for 10 min. Supernatants were collected for HPLC quantification. Expecting DexSP to be metabolized by the ocular tissues into dexamethasone (Dex) (González-Fernández et al., 2023), all samples were analyzed twice by HPLC to detect both DexSP and Dex. The amount of drug extracted was compared to the amount of DexSP initially applied.

At the end of the *in vivo* experiment, the ocular tissues were isolated after euthanasia. Firstly, the aqueous humor was collected from the anterior chamber of the eyes with a 1 mL syringe equipped with a 25G needle. Then, the eyes were enucleated and immediately dissected to isolate the cornea, sclera, and vitreous humor. All collected tissues were separately weighted and treated as follows: the cornea and sclera were immersed in 500 μL and 800 μL of extraction medium, respectively; the aqueous humor and vitreous humor were immersed in pure acetonitrile to reach a final concentration of 65 % acetonitrile in the samples. Then, all samples were processed following the validated drug extraction method. Finally, the supernatants were collected and stored at −80 °C until Ultra High-Performance Liquid Chromatography (UPLC) analysis, which was performed detecting both DexSP and Dex.

To evaluate the drug concentration in the tears over time, Schirmer

strips containing the collected tear fluid samples were placed in 150 μL of extraction medium and processed as previously described for the ocular tissues (i.e., 10 min sonication, overnight incubation at 4 °C, 1 min vortex and 10 min centrifugation at 13000 rpm). The supernatants were stored at −80 °C until HPLC analysis.

The remaining amount of drug in the CLs after 6 h of *in vivo* wearing was also quantified at the end of the test. To do this, the CLs were placed in 1 mL of extraction medium for 24 h at room temperature, vortexed for 1 min and centrifuged at 13000 rpm for 10 min. Then, the amount of remaining drug was quantified by HPLC.

HPLC quantification of DexSP and Dex in the tears was performed as in Section 2.2. UPLC analysis of the ocular tissues eluates was performed with a Waters Acquity UPLC H-Class with a Xevo TQD MS System in the Laboratório de Análises of Instituto Superior Técnico. The chromatographic separation was performed with a BEH C18 column (Waters, 1.7 μm, 2.1 × 75 mm) at 40 °C, with a flow rate of 0.5 mL/min. The mobile phase consisted of component A (0.1 % formic acid in water) and component B (0.1 % formic acid in acetonitrile). A gradient elution was applied as follows: 5–100 % B (0–5 min), 100–5 % B (5–6 min), and 5 % B (6–7 min). Electrospray ionization was run in positive mode with the following conditions: source temperature 150 °C; desolvation temperature 500 °C; capillary voltage 0.5 kV. The cone voltage was set at 20 V for Dex and 60 V for the DexSP. Desolvation gas flow was 1000 L/h, while cone gas flow was 50 L/h. Both drugs were monitored for quantification in selected ion recording (SIR) mode using the *m/z* of 396.2 → 373.2 for Dex, and the *m/z* of 517.1 → 124.9 for DexSP. Calibration curves were obtained in the 0.5–40 ng/mL and 0.1–40 ng/mL concentration range for DexSP and Dex, respectively.

2.9.4. Corneal histology

Histological analysis was performed on a portion of the excised corneas to evaluate the effect of the CLs application on the epithelial structure. Briefly, corneas (either treated with DexSP CLs, DexSP + PEN CLs, or untreated taken as control) were isolated from the rabbit eyes and immersed in 1.5 mL of glutaraldehyde solution (3 % glutaraldehyde in 0.1 M sodium cacodylate buffer, pH 7.4) for 3 h to fix the tissues. The procedure was performed immediately after euthanasia, to avoid post-mortem cellular degradation. After fixation, corneas were stored in 1.5 mL of sodium cacodylate buffer. Then, samples were rinsed, post-fixed for 1 h in 1 % *w/v* osmium tetroxide in the same buffer, and dehydrated with graded ethanol passages. Corneal fragments were then subjected to two 15-min passages in propylene oxide and finally embedded in an Epon-Araldite mixture. Semi-thin sections (1 μm thickness) were cut on a Reichert Ultracut II Ultramicrotome (Leica Microsystem - Wetzlar, Germany) equipped with a glass knife, and stained with toluidine blue for light microscope observation. Thin sections were cut with a diamond knife and stained on the grid with uranyl acetate and lead citrate for observation by transmission electron microscope (TEM) on a JEOL 1200-EX apparatus (JEOL USA, Peabody, MA, USA) (Carapeta and do Bem B, McGuinness J, Esteves A, Abecasis A, Lopes A, 2015).

2.10. In vitro-in vivo correlations

In vitro-in vivo correlations (IVIVC) were attempted through Levy plot analysis, representing the percentage of drug released *in vitro* and *in vivo* at predetermined time points on the x- and y-axes, respectively. The drug amount released *in vivo* to the tear fluid was calculated as the cumulative area under the tear fluid concentration–time curve ($AUC_{0\text{-}t}$) at each time point normalized by the theoretical AUC that could be obtained assuming a complete release from the CLs ($AUC_{0\text{-}\infty}$)(Equation (4)).

$$In\ vivo\ drug\ release\ (\%) = \frac{AUC_{0-t}}{AUC_{0-\infty}} \bullet 100 \quad (4)$$

$AUC_{0\text{-}t}$ was calculated from the experimental data applying the trapezoidal rule (Hiratani et al., 2005) and $AUC_{0\text{-}\infty}$ was obtained as follows (Equation (5)):

$$AUC_{0-\infty} = \frac{AUC_{0-6h}}{P_{t=6h}} \bullet 100 \quad (5)$$

$P_{t=6h}$ represents the percentage of drug released at the end of the experiment ($t = 6\ h$) and was calculated as the difference between the average amount of drug loaded on the CLs and the drug amount extracted from each CL at the end of the experiment (Section 2.9.3), normalized by the total drug amount loaded. Regression analysis was carried out using Prism 8.0.1 software (GraphPad, San Diego, CA, USA).

2.11. Statistical analysis

Quantitative data are presented as the mean ± standard deviation. Statistical analysis was performed on Prism 8.0.1 software (GraphPad, San Diego, CA, USA) by *t-test* if two groups were compared, or, in case of multiple groups, by one-way ANOVA with Tukey's multiple comparisons post hoc test. The normality of the variables was previously assessed by the Shapiro–Wilk test. The significance level was set at $p < 0.05$.

3. Results and discussion

3.1. Ex vivo permeability test

The effect of the peptides on drug permeability across the ocular tissues was evaluated *ex vivo*. The conjunctiva was selected as a model tissue as it covers the vast majority of the accessible eye surface, and, due to its wider intercellular space if compared to the cornea, it constitutes an important absorption route for topically applied drugs (Subrizi et al., 2019). A statistical increase in the P_{app} of the drug was observed when DexSP was co-delivered with PEN ($1.3 \pm 0.2\ x10^{-5}$ cm/s *vs* $0.6 \pm 0.3\ x10^{-5}$ cm/s), while the presence of KTP-NH_2 did not cause a relevant change in the P_{app} value ($0.9 \pm 0.3\ x10^{-5}$ cm/s *vs* $0.6 \pm 0.3\ x10^{-5}$ cm/s) (Fig. 2). A comparable two-fold increase in permeability was reported by Cohen-Avrahami *et al.* (Cohen-Avrahami et al., 2012), who co-delivered diclofenac sodium, a non-steroidal anti-inflammatory drug, with PEN across the porcine skin in *ex vivo* tests.

To explore the potential of the use of PEN as a permeability enhancer for a wider range of drugs, the peptide was then tested in the presence of the hydrophobic Dex, with no significant increase in the P_{app} of the drug

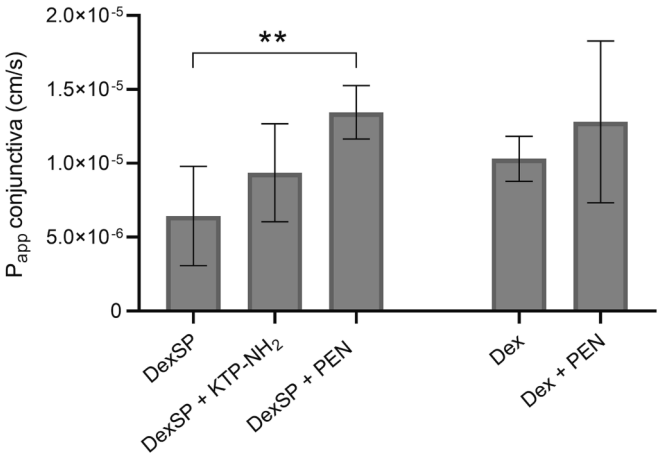

Fig. 2. Apparent permeability of DexSP and Dex across the porcine conjunctiva when administered in solution with either KTP-NH_2 (1:1 drug-peptide ratio) or PEN (10:1 drug-peptide ratio), compared to the permeability of the drugs alone. One-way ANOVA, ** $p < 0.01$ ($n \geq 3$).

(1.3 ± 0.5 x10^{-5} cm/s *vs* 1.0 ± 0.2 x10^{-5} cm/s) (Fig. 2). Interestingly, a recent permeability study by Frøslev *et al.* (Frøslev et al., 2022) across an *in vitro* model of blood–brain barrier also evidenced a dependence of the efficacy of PEN on the cargo properties, namely its hydrophilicity: PEN increased 10-fold the passage of ^{14}C-mannitol, a hydrophilic paracellular flux marker, while resulted ineffective on the P_{app} of ^{3}H-propanolol, a hydrophobic transcellular flux marker.

The reported results are characterized by a wide data dispersion, which is commonly observed when biological tissues are involved. The inter-animal differences, the difficulty in tissue handling and the spatial variability in the selection of the clamped conjunctival area all contribute to the obtained standard deviations. Despite these limitations, *ex vivo* tests are considered a useful tool in comparative studies, and allows for a preliminary screening of numerous drug delivery formulations, thus reducing the need for *in vivo* testing (Agarwal and Rupenthal, 2016).

Given the results obtained, DexSP and PEN were selected for further studies.

3.2. Loading capacity and in vitro drug release

The total amount of DexSP and PEN present in the dual-loaded hydrogels is reported in Fig. 3A. H1 and H2 hydrogels loaded 2.1 ± 0.8 and 1.2 ± 0.4 μg of DexSP per mg of dry hydrogel, respectively, with no significant differences between the two. H3 hydrogel, functionalized with APMA, was able to load a higher amount of DexSP (3.6 ± 0.6 μg/mg of dry hydrogel, $p < 0.05$) due to the affinity of the monomer for the drug. The positive effect of APMA on drug loading, however, was masked when AAc was also included in the hydrogel composition (H4 hydrogel, 1.0 ± 0.1 μg of DexSP/mg dry hydrogel).

AAc, on the other hand, significantly increased ($p < 0.0001$) the amount of PEN loaded in H2 and H4 hydrogels (6.8 ± 0.3 μg/mg and 6.5 ± 0.4 μg/mg of dry hydrogel, respectively) if compared to H1 and H3 (1.4 ± 0.2 μg/mg and 1.2 ± 0.3 μg/mg of dry hydrogel, respectively). Similarly to what was previously observed for DexSP, the presence of AAc was predominant over APMA in the determination of the loading behavior of H4 hydrogel.

The drug and peptide release profiles were then obtained *in vitro* (Fig. 3B, also reported as percentage of the amount loaded in Fig. S7). H3 hydrogel, which was able to load the highest amount of DexSP, also released the highest amount of drug. The presence of APMA as a functional monomer improved the release kinetics and allowed H3 to sustain the delivery of DexSP for at least 24 h. However, the effect of APMA was hindered by AAc presence in H4 hydrogel, which presented a release behavior comparable to H2 hydrogel.

The release profiles of PEN from the four tested hydrogels were comparable. All hydrogels sustained the release of the peptide for about 8 h *in vitro*. H2 and H4 hydrogels, despite the higher amount of PEN loaded, were unable to fully release it in PBS. It is possible that the strong interaction between AAc and PEN resulted in a permanent bond between the functional monomer and the peptide, causing a large fraction of PEN to be trapped in H2 and H4 hydrogels.

Variants in the composition of H3 hydrogel were also tested to reach an equilibrium between APMA and AAc concentrations and tune the

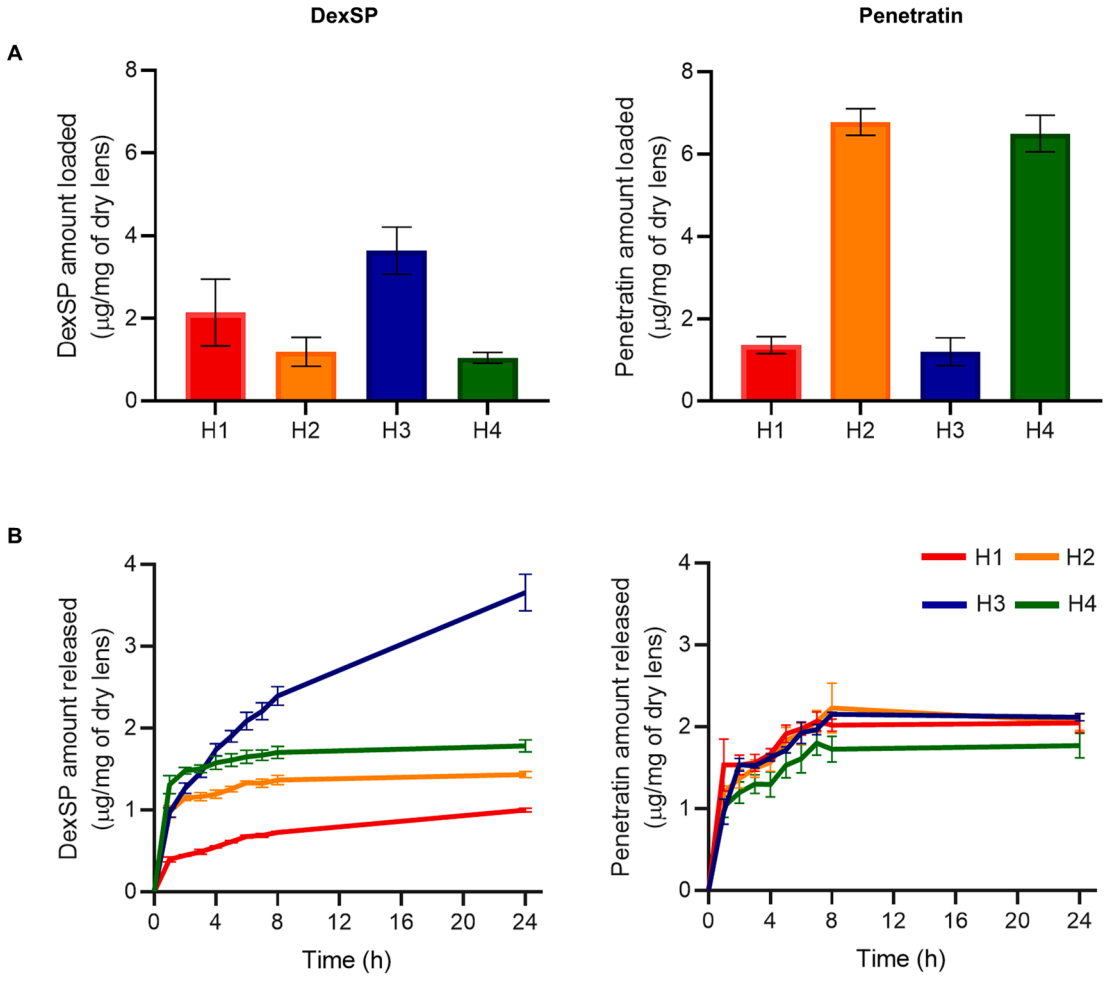

Fig. 3. Amount of drug (left) and peptide (right) loaded into the hydrogel discs by the end of the soaking process (A); simultaneous drug and peptide release profiles from the hydrogels *in vitro*, normalized by the dry weight of the hydrogels (B). Hydrogels composition as in Table 1.

loading and release of both DexSP and PEN (Table S1). However, increasing the amount of APMA (i.e., 200 mM and 300 mM) led to visibly opaque hydrogels, therefore not suitable for optical applications, while decreasing the amount of AAc (i.e., 100 mM) still hindered the interaction of APMA with DexSP (Fig. S8).

Based on the obtained results, H3 hydrogel was selected as the most promising CL material as it allowed for the simultaneous release of DexSP and PEN for at least 8 h, which is compatible with the wearing time of a daily CL.

To investigate the impact of dual loading on the performance of H3 hydrogel as a delivery platform, DexSP and PEN were also individually loaded into the hydrogel. The obtained release profiles are reported in Fig. 4, being compared to the previously observed dual-release curves. While the variation in the release profile of DexSP was negligible, PEN was released from the H3 hydrogel in higher amounts (5-fold increase) when loaded in the presence of the drug. As described in Section 2.4, the amount of drug and peptide loaded into the hydrogels was calculated as the difference in concentration between the external solution at the end of loading and a control solution with no hydrogel. When PEN was individually loaded in H3, no statistical differences were observed in the concentration of the two solutions. This implies a very low amount of peptide individually loaded in H3, which is consistent with the low amount of PEN subsequently released. Besides increasing the amount of PEN loaded, the presence of DexSP in the hydrogel also improved the release kinetics of the peptide. This effect, caused by the molecular interactions of the drug and the peptide not only with the hydrogel matrix but also between each other, was previously reported in studies involving dual-loaded hydrogels (Topete et al., 2019). In this specific case, as PEN is only added during the second loading phase, the increased affinity of the peptide with the hydrogel is probably due to the interaction between the negative charges of DexSP (already present in the hydrogel after the first loading phase) and the positive charges of PEN in solution at pH 7.4.

3.3. Physical characterization

The designed hydrogels were characterized for their wettability, swelling capacity and light transmittance to evaluate their suitability to be used as contact lens materials (Fig. S9).

All hydrogels exhibited a similar wettability, with contact angle values in the range of $33^\circ - 46^\circ$ ($p > 0.05$). Such values indicate the hydrophilic nature of the hydrogels surface, and are comparable to previously reported data for HEMA-based hydrogels (Vivero-Lopez et al., 2021).

The liquid uptake was then evaluated in PBS and at the end of the dual loading procedure. In PBS, H1 hydrogel presented a liquid uptake of 47 ± 2 %, which was not altered ($p > 0.05$) by the addition of APMA as a functional monomer (H3 hydrogel, 52 ± 1 %). Hydrogels H2 and H4, functionalized with AAc, increased their swelling capacity up to 116 ± 1 % and 109 ± 4 %, respectively, due to the increased hydrophilicity of the polymeric matrix.

At the end of the dual loading procedure, the liquid uptake of H1 and H3 hydrogels did not significantly differ from the result obtained in PBS, with a swelling of 54 ± 1 % and 50 ± 2 %, respectively. H2 and H4 hydrogels, instead, further increased their liquid uptake capacity in the presence of the drug and peptide, reaching a final swelling of 136 ± 2 % and 125 ± 7 %, respectively. This effect could be due to the high amount of PEN, which is highly hydrophilic, loaded into H2 and H4 hydrogels (Fig. 3A, a 4-fold increase in PEN content if compared to H1 and H3). Since the water content values reported for commercial contact lenses fall in the 40–70 % range (Tranoudis and Efron, 2004), H1 and H3 hydrogels were considered adequate to be used as CL materials.

Regarding light transmittance, all hydrogels fulfilled the optical requirements as contact lens materials (Rahmani et al., 2014), with values higher than 95 % in the visible range (i.e., between 380 and 700 nm).

3.4. Sterilization

Sterilization of H3 hydrogels in the loading solution was performed by PATP on either the 4th or the 6th day of the loading process. The effect of the sterilization procedure on the release profile *in vitro* is reported in Fig. 5A. The release kinetics of DexSP and PEN was not affected. However, the amount of DexSP released by the hydrogels during 24 h decreased by ≈ 20 % due to sterilization. When sterilization was performed on the 4th day of loading (i.e., at the beginning of the dual loading phase), the amount of peptide released also decreased by ≈ 26 %. This effect was avoided for PEN when PATP was performed on day 6, which was therefore selected as the optimal time point for the sterilization step. The dependence of the drug amount released on the timing of the PATP treatment during the loading procedure has been previously addressed (Topete et al., 2020), and should be experimentally evaluated for each drug/peptide and hydrogel combination.

The comparison between the HPLC spectra of DexSP before and after sterilization confirmed the absence of drug degradation caused by the procedure (Fig. 5B). Circular dichroism analysis did not detect any significant structural change in PEN following PATP. Therefore, sterilization on day 6 of the loading procedure was considered suitable for the drug + peptide-loaded hydrogels.

In view of a scale-up of the CL manufacturing process, the dual-loading could be directly performed in the commercial CL case. The

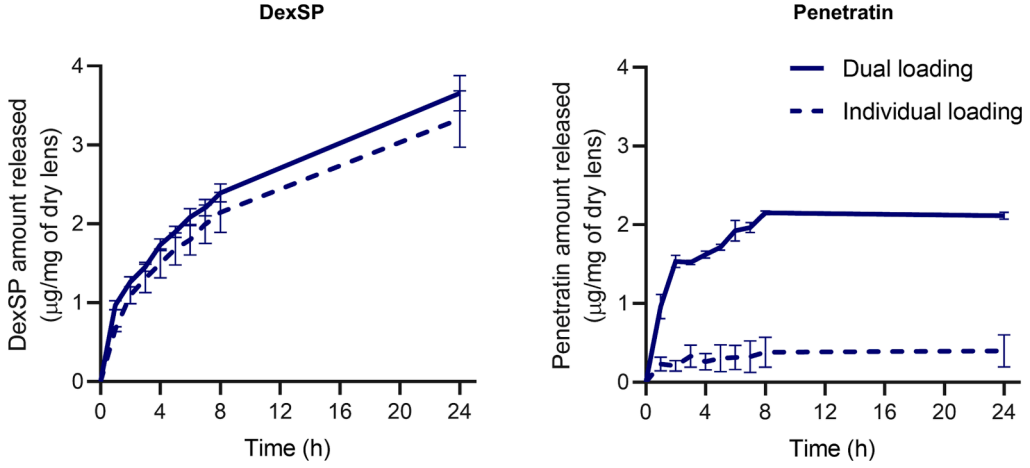

Fig. 4. *In vitro* release profile of DexSP (left) and PEN (right) after dual loading into H3 hydrogel discs, compared to the release profiles of either DexSP or PEN when individually loaded into H3 hydrogel discs.

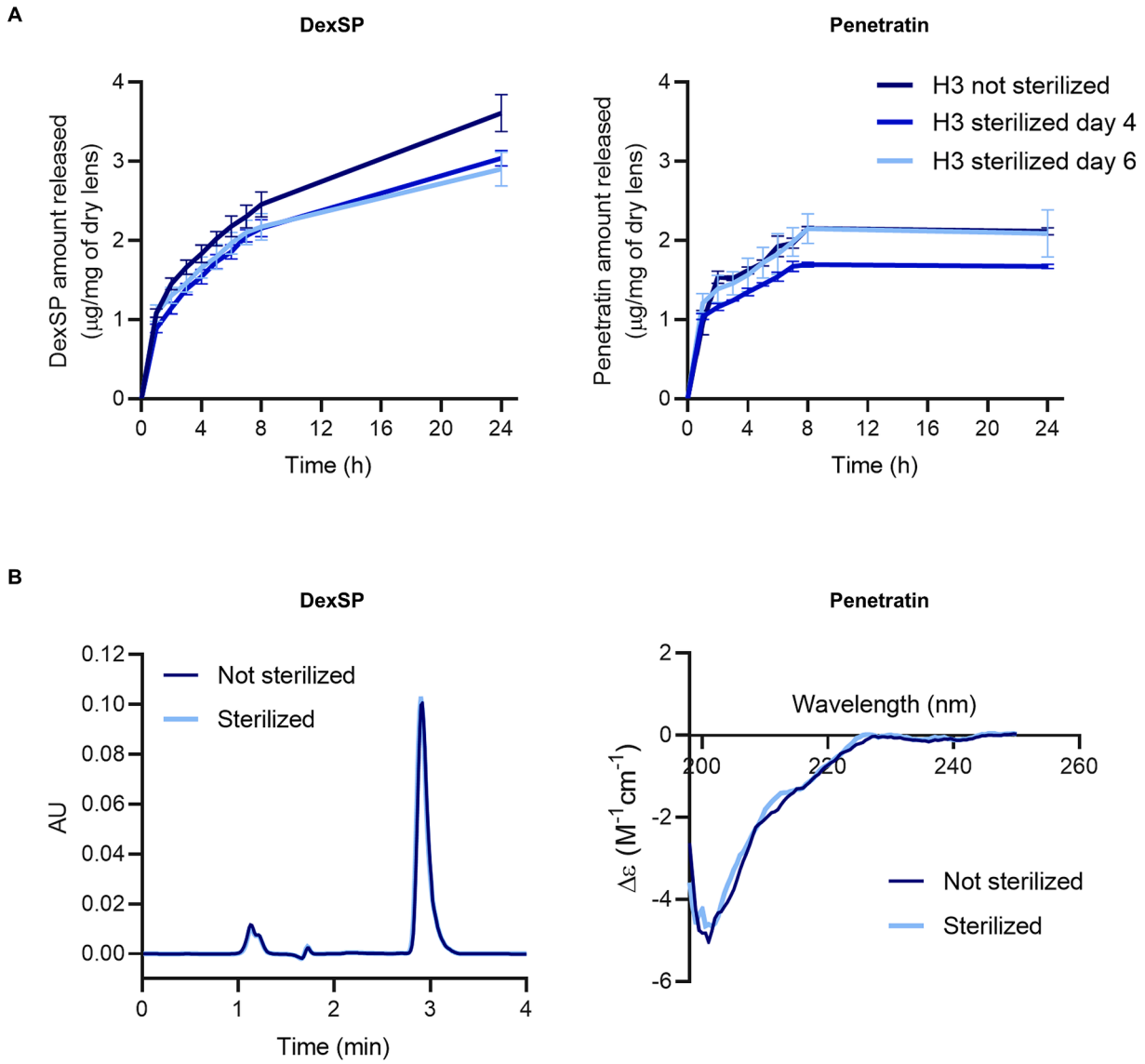

Fig. 5. *In vitro* simultaneous release profile of DexSP (left) and PEN (right) obtained before and after sterilization by PATP (A). The stability of DexSP and PEN after sterilization was assessed by HPLC (left) and CD (right), respectively (B).

use of soft cases or flexible lids would allow for PATP sterilization at the end of the loading phase.

3.5. *In vitro biological characterization*

The viability of primary HCEC was evaluated after exposure to H3 hydrogels either unloaded, to test the material's toxicity, or loaded with both DexSP and PEN to test the therapeutic device. Cell viability resulted equal to 75 ± 6 % and 76 ± 3 % of the negative control after 24 h exposure to the unloaded and loaded hydrogel, respectively (Fig. 6A). Therefore, the designed device was considered non-cytotoxic according to the ISO 10993–5: 2009 standard, which requires minimum cell viability of 70 %.

The HET-CAM test was then performed to predict the irritability potential of loaded H3 hydrogels. The CAM tissue is a recognized model of the ocular mucosal tissues (Budai et al., 2010), as it presents a similar response to irritation. After 5 min of exposure, the IS of the loaded H3 hydrogel resulted equal to 0.35, as opposed to the positive control (IS = 17.45) (Fig. 6B). Therefore, the dual-loaded H3 hydrogel was considered potentially non-irritating for the ocular surface.

The secretion of IL-6, a pro-inflammatory cytokine, from THP-1 cells stimulated with LPS was quantified to evaluate the effect of the presence of PEN and of PATP sterilization on the anti-inflammatory activity of DexSP. A significant reduction (**** $p < 0.0001$) in the IL-6 secretion was observed when cells were pre-treated with DexSP (Fig. 6C), if compared to the positive control. The presence of PEN in the solution (DexSP + PEN) did not reduce the therapeutic activity of the drug. No statistical decrease ($p > 0.05$) in the anti-inflammatory activity was observed between non-sterilized and sterilized (PATP) dual solutions, thus confirming the suitability of the sterilization method.

3.6. *In vivo experiments*

Two systems were tested *in vivo* (i.e., H3 hydrogel-based CLs loaded with DexSP alone, and H3 hydrogel-based CLs loaded with both DexSP and PEN) with the objectives of (i) observing the ocular drug distribution after 6 h wearing of the CLs and (ii) evaluating the efficacy of PEN as a drug carrier across the ocular tissues when simultaneously administered with the drug.

For *in vivo* testing, H3 hydrogel was produced in the shape of CLs (Fig. 7A), loaded with drug and peptide, sterilized, and stored at −20 °C until being used on rabbit eyes. Prior to *in vivo* experiments, the possible

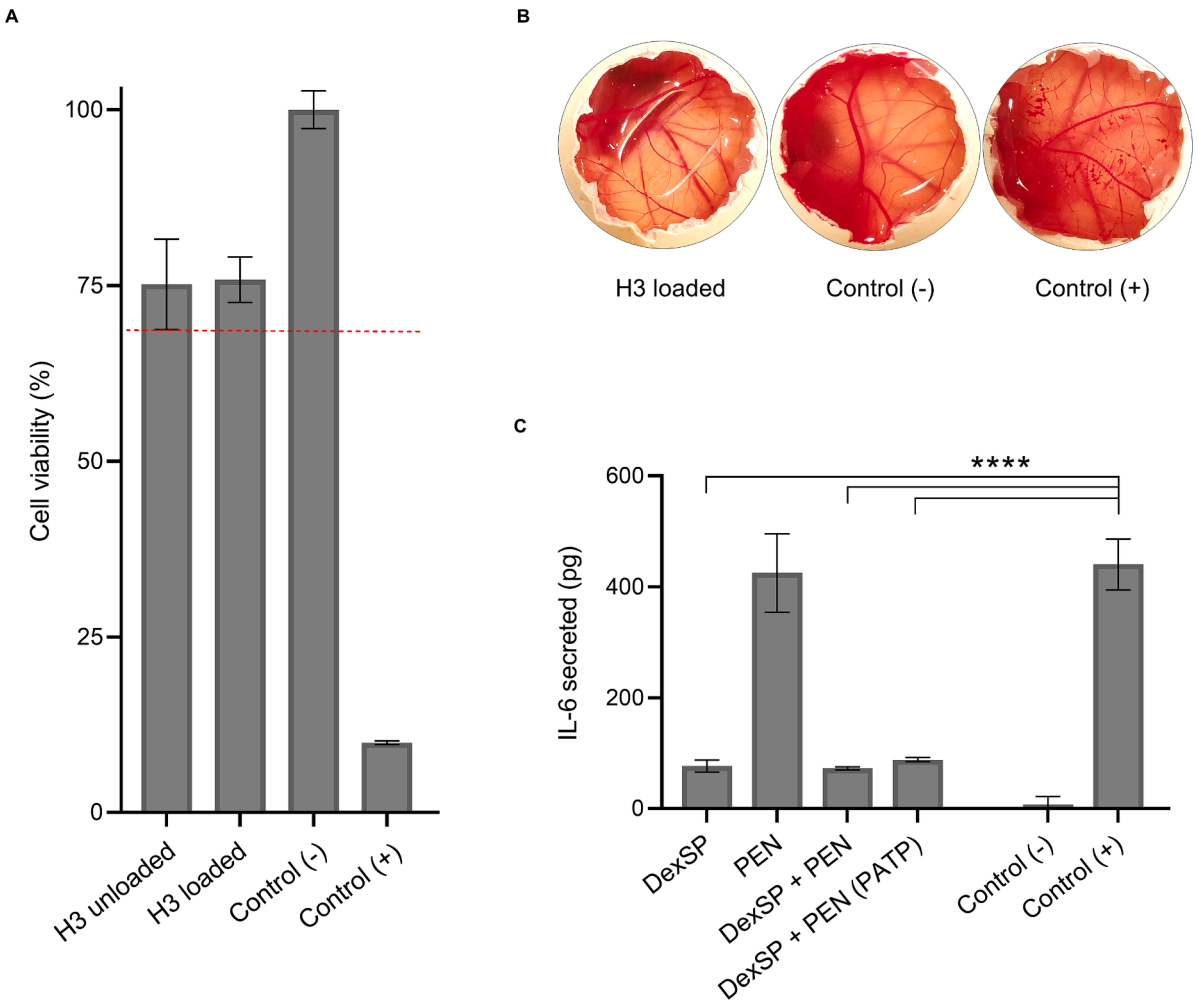

Fig. 6. Cell viability after exposure to unloaded and dual loaded H3 hydrogel, compared to the negative (plain medium) and positive (medium + 10 % DMSO) controls. The minimum cell viability to ensure non-toxicity was set at 70 % of the negative control (red dashed line) (A). HET-CAM images after 5 min of exposure to loaded H3 hydrogels, compared to the negative (0.9 % NaCl) and positive (1 M NaOH) controls (B). Effect of the pre-treatment with DexSP, PEN, or a dual-solution (prior and after PATP sterilization) on the secretion level of IL-6 from THP-1 cells stimulated with LPS, compared to the negative (no LPS) and positive (no pre-treatment) controls (C). n = 4; ANOVA, **** $p < 0.0001$. (For interpretation of the references to colour in this figure legend, the reader is referred to the web version of this article.)

effect of storage, CL composition (i.e., double amount of initiator if compared to discs) and hydrogel shape (i.e., curved CLs *vs* flat discs) was studied. Storage at −20 °C for as long as 10 days was demonstrated not to affect the release profile of either drug or peptide (Fig. S10). If compared to discs, the CLs showed a 25 % reduction in the amount of DexSP released *in vitro* within 6 h of the expected CL wear (Fig. S11A). Differently, no effect was observed on the release of PEN (Fig. S11B). The influence of the higher amount of AIBN, however, resulted negligible in terms of thermal behaviour of the hydrogels: a Tg of 102 ± 3 °C and 102 ± 2 °C was extrapolated from the DSC thermogram of discs and CLs, respectively (Fig. S11C). Similarly, the liquid uptake in PBS showed no significant variation between discs and CLs (52 ± 1 % *vs* 54 ± 1 %, respectively) (Fig. S11D). This suggests a higher influence of the sample surface area-to-volume ratio (≈ 0.35 mm thickness and ≈ 52 mm^3 volume *vs* ≈ 0.3 mm thickness and ≈ 65 mm^3 volume for hydrated discs and CLs, respectively) on the release profile of DexSP, rather than a change in the hydrogel structure due to the amount of AIBN. The fact that the hydrogel shape did not affect the release of PEN was attributed to a loading of PEN only in the external layers of the hydrogel, and not in its bulk. This can be justified with a state of non-equilibrium between the hydrogel and the loading medium after 3 days of PEN loading. Longer loading times, however, are discouraged by the short stability time of PEN in solution (Fig. S3).

The drug concentration in the tears was quantified over time up to 6 h (Fig. 7B), with no significant difference in values between the DexSP group and the DexSP + PEN group. A peak in concentration was registered after 30 min of CL wearing (16 ± 6 μg/mL and 20 ± 11 μg/mL for DexSP delivered alone or with PEN, respectively), which correlates well with the initial burst release from the hydrogels observed *in vitro* during the first hour of immersion in PBS (Fig. 3B). Nonetheless, the sustained release profile observed *in vitro* in the following hours is reflected on the controlled drug concentration obtained *in vivo*, and confirms the suitability of the developed CLs in providing a gradual release throughout the daytime wearing of the device.

The amount of drug accumulated in the ocular tissues was quantified after 6 h of CL wearing. In a preliminary *ex vivo* test, the extraction method was shown to recover at least 90 % of the drug present in the tissues (Fig. S5). The obtained ocular biodistribution *in vivo* is reported in Fig. 7C. As expected, the highest drug concentration was observed in the anterior segment, namely in the cornea, which remained in direct contact with the CL during the experiment, and in the aqueous humor. However, quantifiable drug amounts were also detected in the sclera and vitreous humor, which confirms the possibility of reaching the posterior segment with drug delivery from therapeutic CLs. Similar

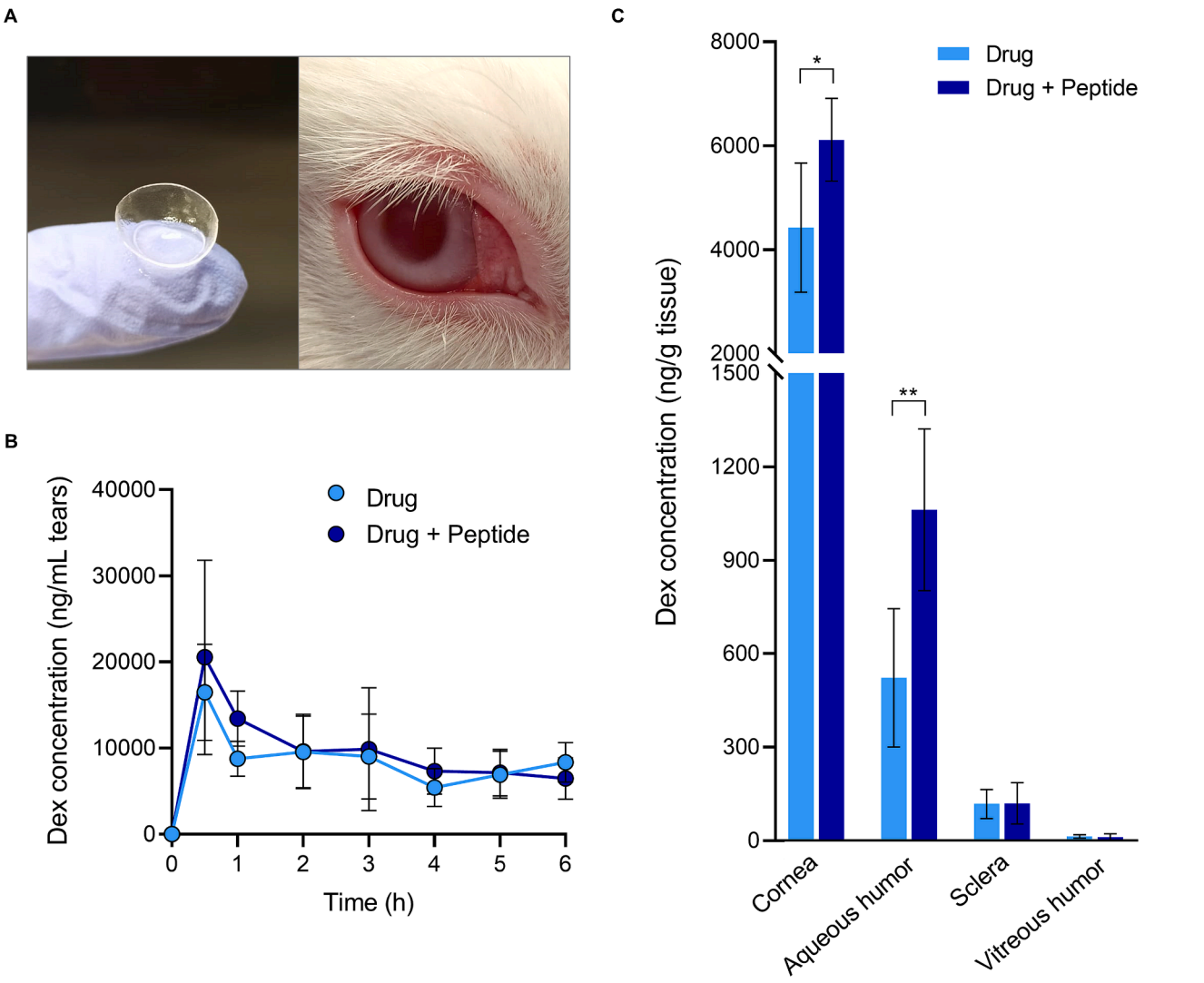

Fig. 7. *In vivo* tests were conducted by placing the developed drug-loaded or drug + peptide-loaded CLs (A, left) on the rabbit eyes below the nictitating membrane (A, right). The obtained CLs contained an average amount of 104.5 μg of DexSP. The concentration of Dex was quantified in the tears over time (B) and in the ocular tissues at t = 6 h (C). n ≥ 5 eyes; *t*-test, * $p < 0.05$; ** $p < 0.01$. The reported data refer to the amount of Dex detected in the tears and ocular tissues. DexSP was metabolized by the ocular tissues and/or hydrolyzed during the CLs wear, being at least 97 % of the drug amount detected in the eluates identified as Dex.

findings were previously obtained with other drug-eluting CLs (Ross et al., 2019; Pereira-da-Mota et al., 2022; Gade et al., 2020). In all the reported studies, the efficiency of drug delivery from CLs to the posterior segment resulted considerably lower than delivery to the anterior segment, due to the barrier effects of the ocular tissues.

The simultaneous delivery of PEN and DexSP, if compared to DexSP alone, significantly increased the drug amount accumulated in the cornea (6114 ± 796 ng *vs* 4423 ± 1241 ng per g of tissue, $p < 0.05$) and aqueous humor (1062 ± 259 ng *vs* 522 ± 222 ng per mL of aqueous humor, $p < 0.01$), thus proving the efficacy of the peptide when used as a drug carrier. Despite the promising results in the anterior segment of the eye, the presence of PEN did not lead to a higher drug accumulation in the posterior segment, with a drug concentration of 118 ± 46 ng/g *vs* 120 ± 66 ng/g in the sclera and 13 ± 5 *vs* 11 ± 10 ng/mL in the vitreous humor, when DexSP was delivered alone or with PEN, respectively.

All data reported in Fig. 7 refer to the amount of Dex detected in the tears and ocular tissues, which constituted at least 97 % of the drug amount detected in the samples. The conversion from DexSP to Dex was attributed to the metabolic activity of the tissues as it was not witnessed *in vitro*. This effect had been previously observed *ex vivo* during the drug extraction test (Fig. S6), and resulted even more noticeable *in vivo* due to the higher metabolic activity of living tissues, if compared to thawed *ex vivo* tissues.

The presence of PEN enhanced the transport of DexSP across the corneal epithelium without disrupting the tissue, as confirmed by histological analysis. No signs of corneal abrasion nor epithelial cell loss were observed in the treated eyes (wearing CLs releasing either DexSP (Fig. 8B) or DexSP + PEN (Fig. 8C)), if compared to the control eye (Fig. 8A).

TEM images of the rabbit corneas were also acquired to identify eventual cell modifications caused by the presence of the peptide. The normal ultrastructural features of the cornea in the control sample (i.e., eyes not treated with the CL) are reported in Fig. 9 A-C: the corneal epithelial cells (Fig. 9A), a keratocyte enveloped into alternating layers of collagen (Fig. 9B) and the characteristic striation of collagen (Fig. 9C), organized into perpendicularly arranged fibers in the adjacent layers. Corneas treated with DexSP-loaded CLs (Fig. 9 D-F) maintained the ultrastructural integrity of the tissue, with no sign of necrotic modification. Mild reversible alterations were indicated by the swelling of the cytoplasmatic organelles in the epithelial cells (vacuoles in Fig. 9D), probably induced by the drug activity. Similar observations are possible for the eyes treated with DexSP + PEN-loaded CLs (Fig. 9G), with no

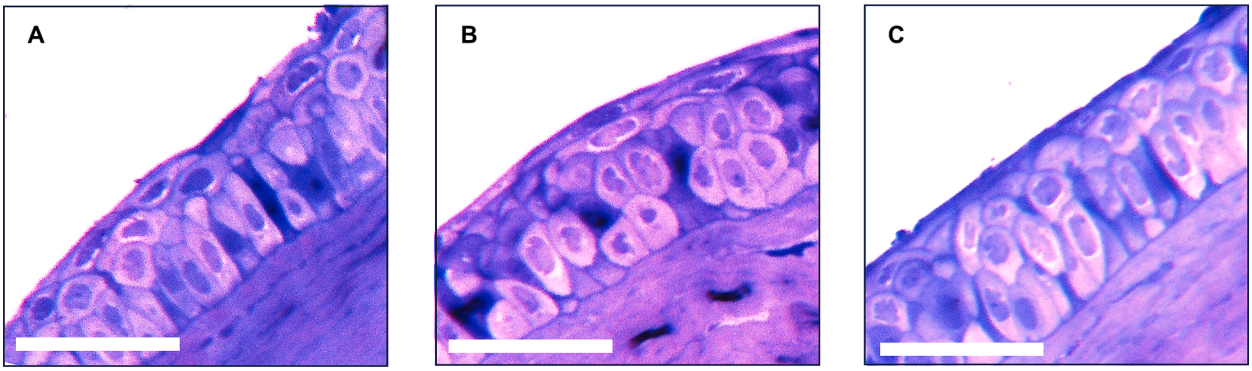

Fig. 8. Optical microscopy images of the rabbit corneal epithelium: untreated eye (A) and treated eyes after 6 h wearing of the developed H3 hydrogel CLs, loaded with either DexSP (B) or DexSP + PEN (C). Scale bar 50 μm.

signs of ulterior alteration caused by the presence of PEN (Fig. 9 H and I).

Overall, a few considerations need to be raised regarding the possibility of using peptides to increase the drug delivery efficiency to the back of the eye after topical drug administration. First, the present study is, to the best of the authors' knowledge, the only reported *in vivo* application of therapeutic CLs simultaneously delivering a cargo drug and a carrier peptide. Although it brings some insight into the potential of using this strategy to overcome the ocular barriers, further investigation would be needed to get more information on the efficacy of the peptide. In particular, it would be useful to measure the drug concentration in the tissues at multiple time points after repeated CL wearing since pathologies affecting the posterior segment of the eye are generally chronic and, therefore, the developed therapeutic CLs are designed for daily application for as long as needed.

Regarding the clinical relevance of the device, a study by Nehmé and Edelman (Nehmé and Edelman, 2008) reported that Dex inhibited the hypersecretion of various inflammatory and angiogenic mediators in stimulated human retinal pericytes, THP-1 monocytes and retinal endothelial cells at doses as low as 1–20 ng/mL (IC_{50}), depending on the tested mediator. Higher doses (400 ng/mL) were suggested for the inhibition of a broader range of pathologic mediators. Even if the drug concentrations detected in the posterior segment after 6 h of CL wearing (i.e., ≈ 120 ng/g and ≈ 13 ng/mL in the sclera and vitreous humor, respectively) did not reach such value, it is possible that repeated CL use may lead to a higher drug accumulation in the posterior segment tissues. Then, as the obtained results evidenced an increased drug transport across the cornea to the aqueous humor, it is reasonable to expect a subsequent drug transport to the adjacent tissues in both the anterior and posterior segment (Toffoletto et al., 2023) and, consequently, an eventual higher drug amount also in the vitreous and retina. Again, repeated CL applications could confirm this hypothesis. Moreover, as the drug amount detected in the vitreous humor and sclera was close to the detection limit of the UPLC equipment, and considering the natural inter-animal variation associated with *in vivo* experiments, it is predictable that more conclusive results would be available after repeated CL use. Safety studies are required to evaluate the performance of the CLs in terms of toxicity and side effects after extended application.

Last, PEN is suggested to act as a carrier for DexSP by establishing a physical association with the drug. The obtained physical complex could be efficient in crossing the first encountered tissues (i.e., the corneal epithelium and the conjunctiva), but, afterwards, this association may be overcome by other interactions, as those between the drug/peptide and the various ocular tissues. A covalent association between the peptide and the drug could help overcome this limitation, and has been reported for other carrier-cargo combinations for ophthalmic applications (Jain et al., 2015; Wang et al., 2010). However, the synthesis of a covalent complex implies drug modification and would require stability studies of the obtained molecule at physiological conditions and during CL loading and storage.

Nonetheless, the proposed CLs, simultaneously releasing DexSP and PEN, demonstrated potential as alternative therapeutic devices able to increase the efficiency of drug delivery across the ocular tissues, mainly in the anterior segment of the eye. The wide range of available peptide carriers and the easy-to-implement strategy of simultaneously delivering the carrier and the cargo open the possibility of tuning CLs as platforms for the treatment of a variety of ocular conditions.

3.7. *In vitro-in vivo correlation*

Establishing a correlation between the *in vivo* and *in vitro* behaviour of a new drug-loaded medical device is crucial for its rational design since the early stages of product development.

The obtained CLs loaded an average amount of 104.5 μg of DexSP. At the end of the experiment (t = 6 h), the percentage of drug released *in vivo* ($P_{t=6h}$) resulted equal to 49 ± 10 % and 57 ± 9 % for the drug-loaded and drug + peptide-loaded CLs, respectively, with no statistical difference between the two groups.

The *in vitro* release profile, represented as the percentage of drug release from the total amount of drug loaded, is compared in Fig. 10A to the estimated drug release *in vivo* over time, either from the drug-loaded or drug + peptide-loaded CLs. As expected, considering the previous *in vitro* results (Fig. 4), no statistically significant differences were observed between the release profiles obtained when administering the drug alone or together with the peptide (Fig. 10A). However, the percentage release was higher *in vitro* than *in vivo,* especially for the first hour (35 % *vs* approx. 16 % of drug released). This effect could be caused by the larger volume of the release medium used *in vitro* (3 mL) if compared to the tears (≈ 7 μL), which may produce a higher driving force for drug diffusion from the CL (Vivero-Lopez et al., 2022). It is also possible that this effect was emphasized by an underestimation of the drug amount released *in vivo* at the very beginning of the experiment, since the drug concentration in the tears was measured for the first time only after 30 min of CL wearing, allowing the continuous tears renewal to possibly mask an initial burst release *in vivo* and contributing to an underestimation of the AUC of the concentration–time curve of the tears in the 0–30 min interval (Fig. 7B).

After the first hour, a strong correlation between the *in vitro* and *in vivo* release rate was observed. As reported in Fig. 10B, which represents the Levy plot of the *in vivo/in vivo* percentage release, the correlation coefficient (R^2) is close to 1 for both drug-loaded and drug + peptide-loaded CLs (R^2 = 0.988 and 0.997, respectively). The positive deviation from the slope 1 line (m = 1.17 and 1.32 for the drug-loaded and drug + peptide-loaded CLs, respectively) is in accordance with previously reported studies (Pereira-da-Mota et al., 2022; Zhu et al., 2018).

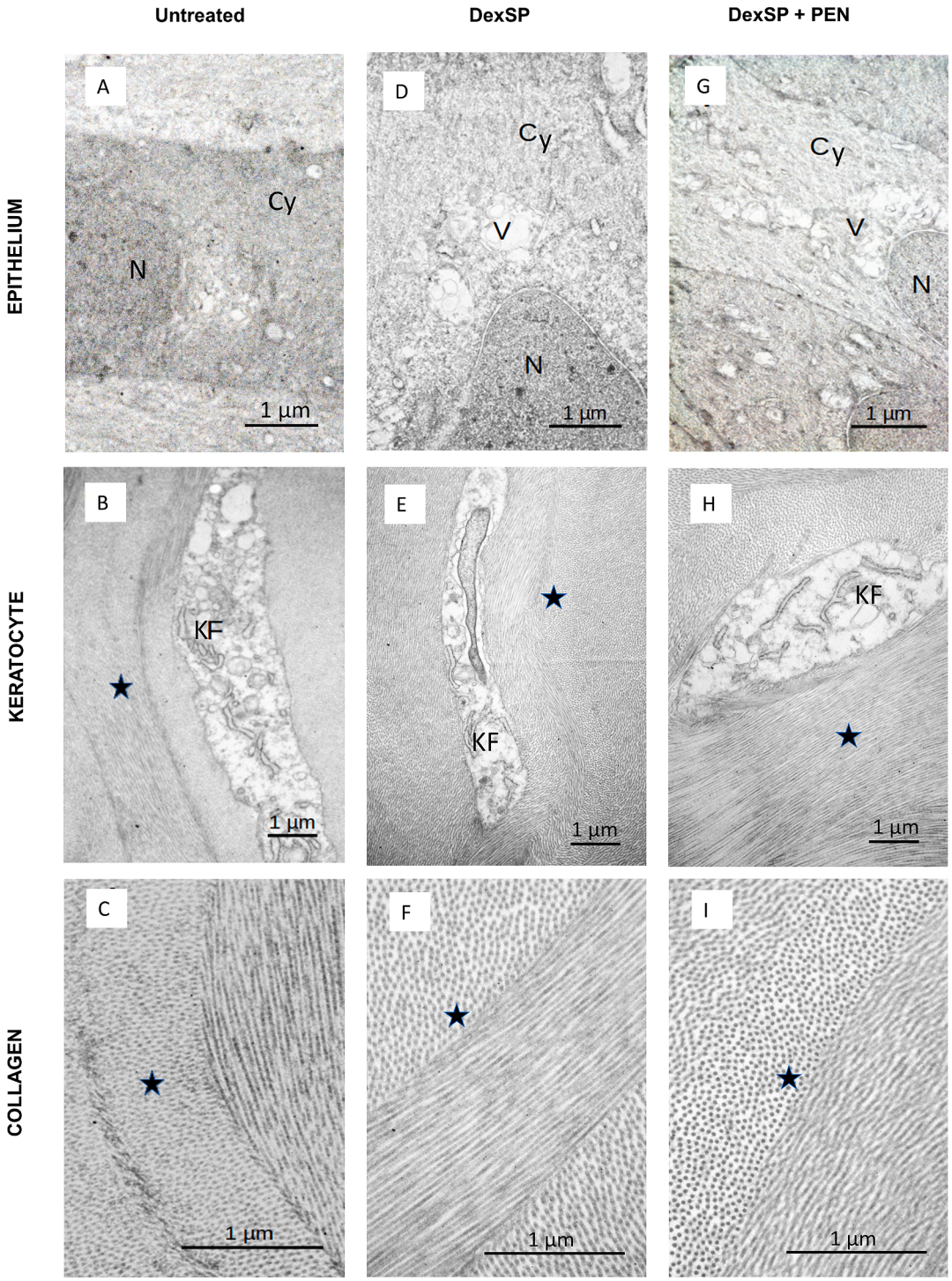

Fig. 9. TEM images of the rabbit cornea: untreated eye (A-C) and treated eyes after 6 h wearing of the developed H3 hydrogel CLs, loaded with either DexSP (D-F) or DexSP + PEN (G-I). Labels: N = nucleus; V = swollen vacuoles; Cy = cytoplasm; ★ = collagen; KF = keratocyte.

4. Conclusion

The possibility of producing hydrogel-based CLs, simultaneously loaded with penetratin and DexSP, acting respectively as carrier and cargo, was evaluated. HEMA-based hydrogels, functionalized with APMA, sustained the release of the peptide and the drug for at least 8 h *in vitro*, consistent with daily CLs' wearing time. The optical properties of the hydrogels and the liquid uptake were considered appropriate for their application as CL materials. The obtained device proved to be non-toxic and biocompatible *in vitro*. *In vivo* tests performed on rabbits revealed a significant increase ($p < 0.05$) in the drug amount detected in the cornea and aqueous humor when DexSP was administered in the presence of penetratin. The developed CLs could increase the drug bioavailability in the internal ocular tissues and contribute to substitute or, at least, minimize the use of intraocular injections. Further investigation, including repeated CL wearing, would be needed to better simulate the clinical use of the device, as pathologies affecting the posterior segment of the eye are generally chronic.

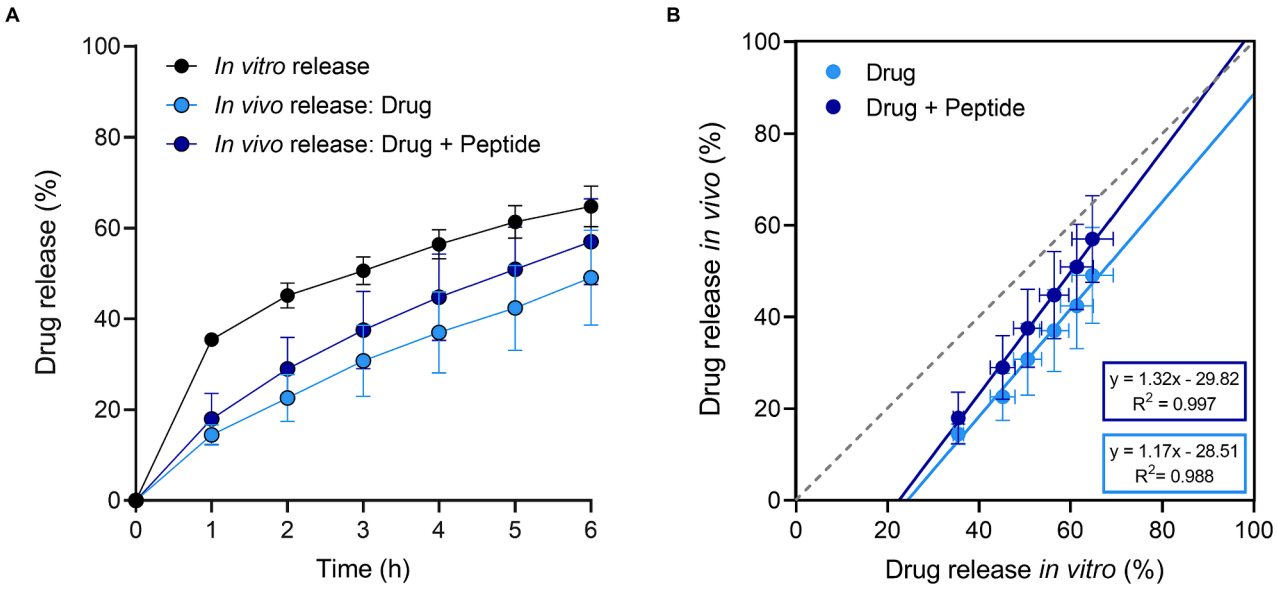

Fig. 10. Comparison between the DexSP release profiles obtained *in vitro* (n = 3, release in 3 mL PBS) and estimated *in vivo* from either drug-loaded or drug + peptide-loaded CLs, calculated from the drug concentration in the tears (n = 5) (A). Levy plot of the IVIVC, where the slope 1 is reported as a grey dotted line (B).

CRediT authorship contribution statement

Nadia Toffoletto: Conceptualization, Methodology, Validation, Formal analysis, Data curation, Investigation, Writing – original draft, Writing – review & editing. **Madalena Salema-Oom:** Methodology, Investigation, Writing – review & editing. **Sara Nicoli:** Supervision, Methodology, Writing – review & editing. **Silvia Pescina:** Methodology, Writing – review & editing. **Felipe M. González-Fernández:** Investigation, Writing – review & editing. **Carlos A. Pinto:** Resources, Writing – review & editing. **Jorge A. Saraiva:** Resources, Writing – review & editing. **António P. Alves de Matos:** Methodology, Investigation, Writing – review & editing. **Maria Vivero-Lopez:** Methodology, Investigation, Writing – review & editing. **Fernando Huete-Toral:** Methodology, Writing – review & editing. **Gonzalo Carracedo:** Supervision, Methodology, Writing – review & editing. **Benilde Saramago:** Conceptualization, Resources, Funding acquisition, Supervision, Writing – review & editing. **Ana Paula Serro:** Conceptualization, Project administration, Resources, Funding acquisition, Supervision, Writing – review & editing.

Declaration of competing interest

The authors declare that they have no known competing financial interests or personal relationships that could have appeared to influence the work reported in this paper.

Data availability

Data will be made available on request.

Acknowledgments

This project has received funding from the European Union's Horizon 2020 research and innovation programme under the Marie Skłodowska-Curie grant agreement N° 813440 (ORBITAL—Ocular Research by Integrated Training and Learning) and is also supported by Fundação para a Ciência e a Tecnologia (FCT) through N. Toffoletto PhD Grant 2022.10004.BD and through the projects UID/QUI/00100/2019, UIDB/00100/2020, UID/BIM/04585/2020, UIDP/00100/2020, IMS-LA/P/0056/2020 and PTDC/CTM-CTM/2353/2021. Thanks are due to the University of Aveiro and FCT/MCTES (Fundação para a Ciência e Tecnologia e Ministério da Ciencia, Tecnologia e Ensino Superior) for the financial support for the LAQV research unit through the projects UIDB/50006/2020 and UIDP/50006/2020. The authors acknowledge Dr. Isabel Correia from Instituto Superior Técnico (IST) for the CD measurements, Carolina Costa (IST) for the support with animal testing, and Dr. Ana Herdade from Faculdade de Medicina da Universidade de Lisboa (FMUL) for the contribution in the research conceptualization. UPLC quantification was performed by Laboratório de Análises do IST (LAIST). The contact lens Teflon molds were produced by Núcleo de Oficinas at IST. The graphical abstract was created using Servier Medical Art by Servier, which is licensed under a Creative Commons Attribution 3.0 Unported License.

Appendix A. Supplementary data

Supplementary data to this article can be found online at https://doi.org/10.1016/j.ijpharm.2023.123685.

References

Agarwal, P., Rupenthal, I.D., 2016. In vitro and ex vivo corneal penetration and absorption models. Drug Deliv. Transl. Res. 6, 634–647. https://doi.org/10.1007/s13346-015-0275-6.

Amit, C., Muralikumar, S., Janaki, S., Lakshmipathy, M., Therese, K.L., Umashankar, V., et al., 2019. Designing and enhancing the antifungal activity of corneal specific cell penetrating peptide using gelatin hydrogel delivery system. Int. J. Nanomed. 14, 605–622. https://doi.org/10.2147/IJN.S184911.

Bhat, A., Smith, B., Dinu, C.Z., Guiseppi-Elie, A., 2019. Dataset on hydrophobicity indices and differential scanning calorimetry thermograms for poly(HEMA)-based hydrogels. Data Br. 24, 103891 https://doi.org/10.1016/j.dib.2019.103891.

Budai, P., Lehel, J., Tavaszi, J., Kormos, É., 2010. HET-CAM test for determining the possible eye irritancy of pesticides. Acta Vet. Hung. 58, 369–377. https://doi.org/10.1556/AVet.58.2010.3.9.

Carapeta, S., do Bem, B., McGuinness, J., Esteves, A., Abecasis, A., Lopes, Â., et al., 2015. Negeviruses found in multiple species of mosquitoes from southern Portugal: Isolation, genetic diversity, and replication in insect cell culture. Virology 483, 318–328. https://doi.org/10.1016/j.virol.2015.04.021.

Cohen-Avrahami, M., Libster, D., Aserin, A., Garti, N., 2012. Penetratin-induced transdermal delivery from H II mesophases of sodium diclofenac. J. Control. Release 159, 419–428. https://doi.org/10.1016/j.jconrel.2012.01.025.

Daoud-Mahammed, S., Grossiord, J.L., Bergua, T., Amiel, C., Couvreur, P., Gref, R., 2008. Self-assembling cyclodextrin based hydrogels for the sustained delivery of hydrophobic drugs. J Biomed Mater Res - Part A 86, 736–748. https://doi.org/10.1002/jbm.a.31674.

de Cogan, F., Hill, L.J., Lynch, A., Morgan-Warren, P.J., Lechner, J., Berwick, M.R., et al., 2017. Topical delivery of anti-VEGF drugs to the ocular posterior segment using cell-penetrating peptides. Invest. Ophthalmol. Vis. Sci. 58, 2578–2590. https://doi.org/10.1167/iovs.16-20072.

Frøslev, P., Franzyk, H., Ozgür, B., Brodin, B., Kristensen, M., 2022. Highly cationic cell-penetrating peptides affect the barrier integrity and facilitates mannitol permeation in a human stem cell-based blood-brain barrier model. Eur. J. Pharm. Sci. 168. https://doi.org/10.1016/j.ejps.2021.106054.

Gade, S.K., Nirmal, J., Garg, P., Venuganti, V.V.K., 2020. Corneal delivery of moxifloxacin and dexamethasone combination using drug-eluting mucoadhesive contact lens to treat ocular infections. Int. J. Pharm. 591, 120023 https://doi.org/10.1016/j.ijpharm.2020.120023.

Ghosh, D., Peng, X., Leal, J., Mohanty, R., 2018. Peptides as drug delivery vehicles across biological barriers. J. Pharm. Investig. 48, 89–111. https://doi.org/10.1007/s40005-017-0374-0.

González-Fernández, F.M., Delledonne, A., Nicoli, S., Gasco, P., Padula, C., Santi, P., et al., 2023. Nanostructured Lipid Carriers for Enhanced Transscleral Delivery of Dexamethasone Acetate: Development, Ex Vivo Characterization and Multiphoton Microscopy Studies. Pharmaceutics 15, 1–22. https://doi.org/10.3390/pharmaceutics15020407.

Gonzalez-Pizarro, R., Parrotta, G., Vera, R., Sánchez-López, E., Galindo, R., Kjeldsen, F., et al., 2019. Ocular penetration of fluorometholone-loaded PEG-PLGA nanoparticles functionalized with cell-penetrating peptides. Nanomedicine 14, 3089–3104. https://doi.org/10.2217/nnm-2019-0201.

Hiratani, H., Fujiwara, A., Tamiya, Y., Mizutani, Y., Alvarez-Lorenzo, C., 2005. Ocular release of timolol from molecularly imprinted soft contact lenses. Biomaterials 26, 1293–1298. https://doi.org/10.1016/j.biomaterials.2004.04.030.

Hsu, K.H., Carbia, B.E., Plummer, C., Chauhan, A., 2015. Dual drug delivery from vitamin e loaded contact lenses for glaucoma therapy. Eur. J. Pharm. Biopharm. 94, 312–321. https://doi.org/10.1016/j.ejpb.2015.06.001.

Hui, A., 2017. Contact lenses for ophthalmic drug delivery. Clin. Exp. Optom. 100, 494–512. https://doi.org/10.1111/cxo.12592.

Jain, A., Shah, S.G., Chugh, A., 2015. Cell penetrating peptides as efficient nanocarriers for delivery of antifungal compound, natamycin for the treatment of fungal keratitis. Pharm. Res. 32, 1920–1930. https://doi.org/10.1007/s11095-014-1586-x.

Johnson, L.N., Cashman, S.M., Kumar-Singh, R., 2008. Cell-penetrating peptide for enhanced delivery of nucleic acids and drugs to ocular tissues including retina and cornea. Mol. Ther. 16, 107–114. https://doi.org/10.1038/sj.mt.6300324.

Johnson, L.N., Cashman, S.M., Read, S.P., Kumar-Singh, R., 2010. Cell penetrating peptide POD mediates delivery of recombinant proteins to retina, cornea and skin. Vision Res. 50, 686–697. https://doi.org/10.1016/j.visres.2009.08.028.

Kim, J., Chauhan, A., 2008. Dexamethasone transport and ocular delivery from poly (hydroxyethyl methacrylate) gels. Int. J. Pharm. 353, 205–222. https://doi.org/10.1016/j.ijpharm.2007.11.049.

Kristensen, M., Franzyk, H., Klausen, M.T., Iversen, A., Bahnsen, J.S., Skyggebjerg, R.B., et al., 2015. Penetratin-Mediated Transepithelial Insulin Permeation: Importance of Cationic Residues and pH for Complexation and Permeation. AAPS J. 17, 1200–1209. https://doi.org/10.1208/s12248-015-9747-3.

Lorenzo-Veiga, B., Diaz-Rodriguez, P., Alvarez-Lorenzo, C., Loftsson, T., Sigurdsson, H. H., 2020. In Vitro and Ex Vivo Evaluation of Nepafenac-Based Cyclodextrin Microparticles for Treatment of Eye Inflammation. Nanomaterials 10. https://doi.org/10.3390/nano10040709.

Malakooti, N., Alexander, C., Alvarez-Lorenzo, C., 2015. Imprinted Contact Lenses for Sustained Release of Polymyxin B and Related Antimicrobial Peptides. J. Pharm. Sci. 104, 3386–3394.

Maulvi, F.A., Soni, T.G., Shah, D.O., 2015. Extended Release of Timolol from Ethyl Cellulose Microparticles Laden Hydrogel Contact Lenses. Open Pharm Sci J 2, 1–12. https://doi.org/10.2174/1874844901502010001.

Moiseev, R.V., Morrison, P.W.J., Steele, F., Khutoryanskiy, V.V., 2019. Penetration enhancers in ocular drug delivery. Pharmaceutics 11. https://doi.org/10.3390/pharmaceutics11070321.

Nehmé, A., Edelman, J., 2008. Dexamethasone inhibits high glucose-, TNF-α- And IL-1β-induced secretion of inflammatory and angiogenic mediators from retinal microvascular pericytes. Invest. Ophthalmol. Vis. Sci. 49, 2030–2038. https://doi.org/10.1167/iovs.07-0273.

Olajide, O.A., Iwuanyanwu, V.U., Lepiarz-Raba, I., Al-Hindawi, A.A., 2021. Induction of Exaggerated Cytokine Production in Human Peripheral Blood Mononuclear Cells by a Recombinant SARS-CoV-2 Spike Glycoprotein S1 and Its Inhibition by Dexamethasone. Inflammation 44, 1865–1877. https://doi.org/10.1007/s10753-021-01464-5.

Pereira-da-Mota, A.F., Vivero-Lopez, M., Serramito, M., Diaz-Gomez, L., Serro, A.P., Carracedo, G., et al., 2022. Contact lenses for pravastatin delivery to eye segments: Design and in vitro-in vivo correlations. J. Control. Release 348, 431–443. https://doi.org/10.1016/j.jconrel.2022.06.001.

Pescina, S., Ostacolo, C., Gomez-Monterrey, I.M., Sala, M., Bertamino, A., Sonvico, F., et al., 2018. Cell penetrating peptides in ocular drug delivery: State of the art. J. Control. Release 284, 84–102. https://doi.org/10.1016/j.jconrel.2018.06.023.

Pescina, S., Lucca, L.G., Govoni, P., Padula, C., Del Favero, E., Cantù, L., et al., 2019. Ex vivo conjunctival retention and transconjunctival transport of poorly soluble drugs using polymeric micelles. Pharmaceutics 11. https://doi.org/10.3390/pharmaceutics11090476.

Pescina, S., Sala, M., Scala, M.C., Santi, P., Padula, C., Campiglia, P., et al., 2020. Synthesis and ex vivo trans-corneal permeation of penetratin analogues as ophthalmic carriers: Preliminary results. Pharmaceutics 12, 1–10. https://doi.org/10.3390/pharmaceutics12080728.

Rahmani, S., Mohammadi Nia, M., Akbarzadeh Baghban, A., Nazari, M.R., Ghassemi-Broumand, M., 2014. Spectral transmittance of UV-blocking soft contact lenses: A comparative study. Contact Lens Anterior Eye 37, 451–454. https://doi.org/10.1016/j.clae.2014.07.011.

Ribeiro, M.M.B., Pinto, A., Pinto, M., Heras, M., Martins, I., Correia, A., et al., 2011. Inhibition of nociceptive responses after systemic administration of amidated kyotorphin. Br. J. Pharmacol. 163, 964–973. https://doi.org/10.1111/j.1476-5381.2011.01290.x.

Ross, A.E., Bengani, L.C., Tulsan, R., Maidana, D.E., Salvador-Culla, B., Kobashi, H., et al., 2019. Topical sustained drug delivery to the retina with a drug-eluting contact lens. Biomaterials 217. https://doi.org/10.1016/j.biomaterials.2019.119285.

Silva, D., de Sousa, H.C., Gil, M.H., Santos, L.F., Amaral, R.A., Saraiva, J.A., et al., 2021. Imprinted hydrogels with LbL coating for dual drug release from soft contact lenses materials. Mater. Sci. Eng. C 120, 111687. https://doi.org/10.1016/j.msec.2020.111687.

Subrizi, A., del Amo, E.M., Korzhikov-Vlakh, V., Tennikova, T., Ruponen, M., Urtti, A., 2019. Design principles of ocular drug delivery systems: importance of drug payload, release rate, and material properties. Drug Discov. Today 24, 1446–1457. https://doi.org/10.1016/j.drudis.2019.02.001.

Thareja, A., Hughes, H., Alvarez-lorenzo, C., Hakkarainen, J.J., Ahmed, Z., 2021. Penetration enhancers for topical drug delivery to the ocular posterior segment — a systematic review. Pharmaceutics 13, 1–17. https://doi.org/10.3390/pharmaceutics13020276.

Toffoletto, N., Salema-Oom, M., Igea, S.A., Alvarez-Lorenzo, C., Saramago, B., Serro, A. P., 2021. Drug-loaded hydrogels for intraocular lenses with prophylactic action against pseudophakic cystoid macular edema. Pharmaceutics 13. https://doi.org/10.3390/pharmaceutics13070976.

Toffoletto, N., Saramago, B., Serro, A.P., 2021. Therapeutic Ophthalmic Lenses : A Review. Pharmaceutics 13 (1), 1–33. https://doi.org/10.3390/pharmaceutics13010036.

Toffoletto, N., Saramago, B., Serro, A.P., Chauhan, A., 2023. A Physiology-Based Mathematical Model to Understand Drug Delivery from Contact Lenses to the Back of the Eye. Pharm. Res. https://doi.org/10.1007/s11095-023-03560-7.

Tomani, J.C.D., Kagisha, V., Tchinda, A.T., Jansen, O., Ledoux, A., Vanhamme, L., et al., 2020. The inhibition of NLRP3 inflammasome and IL-6 production by hibiscus noldeae baker f. derived constituents provides a link to its anti-inflammatory therapeutic potentials. Molecules 25, 1–16. https://doi.org/10.3390/molecules25204693.

Topete, A., Serro, A.P., Saramago, B., 2019. Dual drug delivery from intraocular lens material for prophylaxis of endophthalmitis in cataract surgery. Int. J. Pharm. 558, 43–52. https://doi.org/10.1016/j.ijpharm.2018.12.028.

Topete, A., Pinto, C.A., Barroso, H., Saraiva, J.A., Barahona, I., Saramago, B., et al., 2020. High Hydrostatic Pressure as Sterilization Method for Drug-Loaded Intraocular Lenses. ACS Biomater Sci. Eng. 6, 4051–4061. https://doi.org/10.1021/acsbiomaterials.0c00412.

Tranoudis, I., Efron, N., 2004. Water properties of soft contact lens materials. Contact Lens Anterior Eye 27, 193–208. https://doi.org/10.1016/j.clae.2004.08.003.

Vivero-Lopez, M., Muras, A., Silva, D., Serro, A.P., Otero, A., Concheiro, A., et al., 2021. Resveratrol-loaded hydrogel contact lenses with antioxidant and antibiofilm performance. Pharmaceutics 13. https://doi.org/10.3390/pharmaceutics13040532.

Vivero-Lopez, M., Pereira-Da-Mota, A.F., Carracedo, G., Huete-Toral, F., Parga, A., Otero, A., et al., 2022. Phosphorylcholine-Based Contact Lenses for Sustained Release of Resveratrol: Design, Antioxidant and Antimicrobial Performances, and in Vivo Behavior. ACS Appl. Mater. Interfaces 14, 55431–55446. https://doi.org/10.1021/acsami.2c18217.

Wang, C.Y., Huang, H.W., Hsu, C.P., Yang, B.B., 2016. Recent Advances in Food Processing Using High Hydrostatic Pressure Technology. Crit. Rev. Food Sci. Nutr. 56, 527–540. https://doi.org/10.1080/10408398.2012.745479.

Wang, Y., Lin, H., Lin, S., Qu, J., Xiao, J., Huang, Y., et al., 2010. Cell-penetrating peptide TAT-mediated delivery of acidic FGF to retina and protection against ischemia-reperfusion injury in rats. J. Cell Mol. Med. 14, 1998–2005. https://doi.org/10.1111/j.1582-4934.2009.00786.x.

Xia, H., Gao, X., Gu, G., Liu, Z., Hu, Q., Tu, Y., et al., 2012. Penetratin-functionalized PEG-PLA nanoparticles for brain drug delivery. Int. J. Pharm. 436, 840–850. https://doi.org/10.1016/j.ijpharm.2012.07.029.

Zhang, Z., Huang, W., Lei, M., He, Y., Yan, M., Zhang, X., et al., 2016. Laser-triggered intraocular implant to induce photodynamic therapy for posterior capsule opacification prevention. Int. J. Pharm. 498, 1–11. https://doi.org/10.1016/j.ijpharm.2015.10.006.

Zhu, Q., Cheng, H., Huo, Y., Mao, S., 2018. Sustained ophthalmic delivery of highly soluble drug using pH-triggered inner layer-embedded contact lens. Int. J. Pharm. 544, 100–111. https://doi.org/10.1016/j.ijpharm.2018.04.004.